INTERNATIONAL ATOMIC ENERGY AGENCY
UNITED NATIONS EDUCATIONAL, SCIENTIFIC AND CULTURAL ORGANIZATION

INTERNATIONAL CENTRE FOR THEORETICAL PHYSICS
34100 TRIESTE (ITALY) - P.O.B. 586 - MIRAMARE - STRADA COSTIERA 11 - TELEPHONES: 224281/2/3/4/5/6
CABLE: CENTRATOM - TELEX 46392 ICTP

SMR-30/ 40

WINTER COLLEGE ON ATOMIC AND MOLECULAR PHYSICS

26 January - 18 March 1977

BACKGROUND MATERIALS FOR LECTURES OF

F. DE MARTINI
Istituto di Fisica
Università di Roma
Italy

These are preliminary lecture notes intended for participants only. Extra copies are available outside the Publications Office (T-floor) or from room 112.

P. SOROKIN

Volume 9, number 2 OPTICS COMMUNICATIONS October 1973

ELECTRIC-FIELD INDUCED NONLINEAR COHERENT INFRARED SPECTROSCOPY INVESTIGATION OF THE $Q_{01}(1)$ VIBRO-ROTATIONAL MODE OF THE H_2 MOLECULE[☆]

F. CAPASSO and F. De MARTINI

Istituto di Fisica "G. Marconi", Università di Roma, Rome, Italy

Received 25 July 1973

A new method of nonlinear spectroscopy has been applied to the investigation of the $Q_{01}(1)$ (Raman active) transition of the H_2 molecule. The method has been applied to the first *direct* measurement of the T_2 coherence relaxation time in a gaseous medium, by a coherent Transient Free-induction decay effect.

Several authors have reported in the last decade the application to spontaneous optical spectroscopy of the effect of inducing, by an applied static field E_0, an electric dipole moment μ for those eigenmodes of the system under study for which this one is zero in absence of perturbations [1, 2]. This can be ascribed, in many cases, to the obvious selection rule related to the equal parity of the couple of levels involved, if this quantity is a good quantum number [3]. If this is the case (and other selection rules do not interfere [4]) the corresponding "totally symmetric" mode is in turn Raman active or, more generally, active for a two-photon decay or absorption process [5]. In nonlinear optics little attention has been paid in the past to the E-field induction effect which is always a relatively small effect but, we believe, may be extremely useful for the investigation of several properties of the system under study, such as measurement of physical (linear and nonlinear) parameters and the detection of processes of physical significance [5, 6]. Our present work is somewhat related to work [6] in which the E-field induced ir emission was detected during a Stimulated Raman Scattering (SRS) process. However we shall see that the significant part of our work does not deal properly with SRS, which involves threshold and high gain effects in relatively dense media, but rather with the 2-photon Coherent Excitation (CE) process, a nonlinear mixing effect (no threshold involved) first introduced several years ago [7, 8] and which, since then, has been at the basis of several new useful methods of nonlinear molecular and solid-state spectroscopy [9–11]. The experimental set-up is shown in fig. 1. A ruby laser, Q-switched by a rotating prism and working on a single axial mode (linewidth $\lesssim 0.01$ cm^{-1}) was the pump of a H_2 (SRS) oscillator A in which the pressure of the gas could be varied over about an order of magnitude. The laser pulses were 15 nsec of duration, 30 MW of power. The Stokes oscillator A, composed by a gas cell in which the pump beam was focused by a 15 cm $f/1$ lens, could easily be tuned over a substantial frequency range owing to the pressure-induced Raman shift effect [12]. If ω_0 is the center frequency of the $Q_{01}(1)$ resonance of H_2 which is active in SRS [13], it may be represented in terms of the gas density ρ by the expression

$$\omega_0 = \bar{\omega}_0 + (a\rho + b\rho^2),$$

where $\bar{\omega}_0$ is the Raman shift at $\rho = 0$ and $a = -3.2 \times 10^{-3}$ cm^{-1}/am at $T = 300$ K. The quadratic term $b\rho^2$ is found to be negligible for $\rho \leqslant 80$ amagat [14]. The laser + Stokes beams emerging from A were superimposed by a further $10f/1$ lens in the (test) cell B in which a static field E_0 was created, in the focal region of the beams, by a couple of electrodes connected to a high-voltage cw power supply. During our experiments, in B the pressure of the H_2 gas was set to values generally very low and always less than 1 atm. This created two experimental problems:

a) The difference between the pressures in A and B resulted in a substantial mismatch of the resonant frequencies owing to the pressure-induced line shift effect

---

[☆] Work supported by G.N.S.M.–C.N.R.

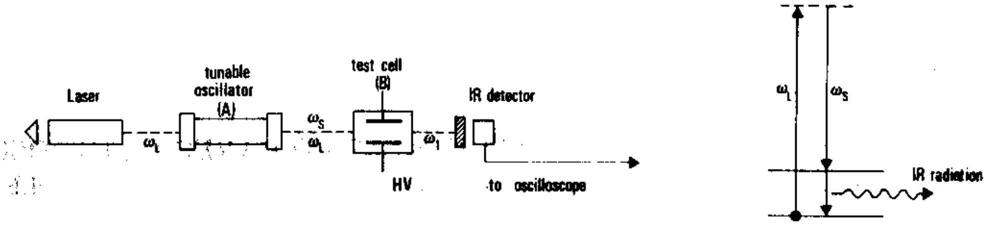

Fig. 1. Schematic diagram of the experimental apparatus.

we have just mentioned. In order to resonantly excite the H_2 molecules in B we had to resort to the effect of mixing H_2 with foreign gases, an effect we made use of in a recent work [11].

b) At low pressures the dielectric strength of the gas decreases, following the Paschen law. For metallic electrodes freely immersed in the gas, discharge streams started from the electrode borders at values of E_0 that were too low in order to achieve a sizable conversion in the infrared. We partially overcame this problem by screening the surface of the electrodes by sheets of teflon. Further details on the appratus will be given in a following, more extended paper. The optical beams emerging from A and B were filtered out by a Ge plate and by an interference filter centered on the $Q_{01}(1)$ Raman shift of $H_2 : \omega_0 = 4155.21 \text{ cm}^{-1}$ and corresponding to a wavelength $\lambda = 2.41$ μm. The coherent infrared field at this frequency was detected by an ultrafast InAs detector coupled to a Fairchild μA 733C fast preamplifier. The signals were further recorded by an oscilloscope.

Before discussing the results of our experiment it seems worthwhile to discuss briefly some physical processes underlying the effect we are investigating. The infrared coherent beam we are detecting arises from the parametric three-wave resonant mixing effects sketched in the right-hand side part of fig. 1. The coupling between the ω_L, ω_s fields and the $\omega_{IR} \equiv \omega_0$ emitted field is provided by the E_0 field induced dipole moment $\langle\mu\rangle_{01} = E_0\alpha_{01}$ which gives rise to two different physical effects: a linear one consisting of the appearance of an (induced) resonant absorption effect, and a nonlinear one resulting in the three-wave coupling. The expression of the absorption coefficient $\kappa''(\nu)$ near resonance may be given in the following form [3]:

$$\kappa''(\nu) = \frac{8\pi^3 \nu_0 \rho |\langle\mu\rangle_{01}|^2}{hc} S(\nu),$$

where $S(\nu)$ is the line-shape factor and c the gas density expressed in molecules/cc. For lorentzian and gaussian lines $S(\nu)$ is given respectively by

$$S(\nu) = \frac{\Delta\nu/\pi}{(\nu-\nu_0)^2 + (\Delta\nu)^2}$$

and

$$S(\nu) = \sqrt{\frac{\ln 2}{\pi(\Delta\nu)^2}} \exp\left[-\frac{\nu-\nu_0}{\Delta\nu}\sqrt{\ln 2}\right].$$

2

The maximum value of κ_1'' in either cases is:

$$\kappa_1''(\nu_0) = \frac{4\pi}{\hbar c}\left(\frac{\nu_0}{\Delta\nu}\right)|\langle\mu\rangle_{01}|^2\rho$$

(Lorentzian) and

$$\kappa_1''(\nu_0) = \frac{4\pi^2}{\hbar c}\sqrt{\frac{\ln 2}{\pi}}\left(\frac{\nu_0}{\Delta\nu}\right)|\langle\mu\rangle_{01}|^2\rho$$

(Gaussian). Assuming the data on induced absorption reported in [2] for the $Q_{01}(1)$ line of H_2, $\alpha_{01} = 1.2 \times 10^{-25} \text{ cm}^3$ and $|\langle\mu\rangle_{01}|^2 = 8 \times 10^{-46}$ u.e.s. for $E_0 = 70$ kV/cm. Finally we obtain

$$\kappa_1''(\nu_0) = 3.75 \times 10^{-3} \text{ cm}^{-1}$$

having assumed a lorentzian line at 1 atm [11], $E_0 = 70$ kV/cm.

The explicit expression of the nonlinear parameter accounting for the three-wave parametric coupling $\beta_{12}(\nu)$ must be evaluated by quantum-mechanical perturbation theory of the nonlinear optical polarizabilities [15, 16]. If $\beta_{12}(\nu_0)$ and $\kappa_1''(\nu_0)$ are small, as in our case, we may nevertheless make use of an useful relation existing between these quantities and the gain G of the S.R.S. effect corresponding to the same resonance [16]:

$$|\beta_{12}^{(\nu_0)}|^2 = \kappa_1''(\nu_0)G(\nu_0)/2$$

in resonance. The dynamics of the three-wave interaction near Raman resonance has been thoroughly considered in [11] and [16]. The spatial evolution of the infrared intensity $\mathcal{E}_1(z)$ along the active path z in the cell B is given in terms of the intensity of the interacting optical fields at the entrance of the cell $z = 0$, $\mathcal{E}_2(0)$, $\mathcal{E}_3(0)$ by the following expression, valid in case of no depletion on the pump

$$\mathcal{E}_1(z) \equiv |E_1(z)|^2$$

$$= \frac{4|\beta_{12}^{(\nu)}|^2 \mathcal{E}_2(0)}{G(1-\vartheta)} \{\exp[\tfrac{1}{2} G(1-\vartheta) z] - 1\}^2 . \qquad (1)$$

In our case $\vartheta \equiv 2\kappa_1''(\nu_0)/G(\nu_0)$ is much less than one leading to a quasi-exponential growth of the waves $\mathcal{E}_1(z)$ and $\mathcal{E}_2(z)$ [7, 17]. Applying the quoted relation between linear and nonlinear coupling parameters and expanding to second order the exponential at the r.h.s. of (1) we finally get the simplified expression for the emitted infrared intensity:

$$\mathcal{E}_1(z) = \tfrac{1}{2}\mathcal{E}_2(0)\kappa_1'' G z^2$$

showing a parabolic dependence of $\mathcal{E}_1(z)$ on z. Assuming $E_0 = 20$ kV/cm, $I_3(0) = 500$ MW/cm^2, $\mathcal{E}_2(0) = 1$ MW for an interaction path l of 1 mm, at the gas pressure $p = 1$ atm, we get from the above formula $\mathcal{E}_1(l) = 0.53$ W having assumed the value of $G(\nu_0)$ given in [18]. Before discussing our results it seems worthwile to comment briefly on two effects which may be thought at first sight, to perturb the process of ir emission. The optical dispersion of refraction index of the gas for the interacting frequencies results in limiting the "coherence length" of the interaction [15]. We have evaluated it to be $l_c \approx 15$ cm at $p = 1$ atm, a value well above the length of the focal region in the cell B. We shall further consider that $l_c \propto p^{-1}$. The E_0-field induced Stark shift of the Raman line may be in principle a further source of experimental problems. In effect this process introduced a negligible perturbation. The shift has been evaluated by Terhune and Peters [1] to be of the order of 10^{-4} cm^{-1} for $E_0 = 10$ kV/cm, a value about 50 times less than the forward scattering Dicke-narrowed Raman line. (We should recall here that the maximum forward Dicke-narrowing for the $Q_{01}(1)$ resonance in H_2 corresponds to a gas pressure of about 1 atm [11]).

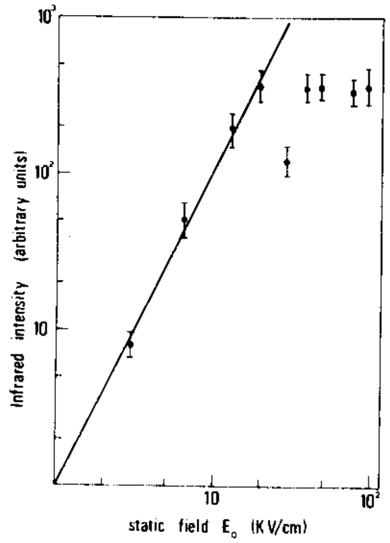

Fig. 2. Plot of the infrared intensity vs. static electric field E_0.

In fig. 2 the experimental plot of the emitted intensity I_1 at $\lambda = 2.4$ µm ($p = 1$ atm) is reported as function of E_0. The behavior shown in fig. 2 corresponds to the expected E_0^2 dependence for $E_0 \lesssim 20$ kV/cm. The experimental values of the intensity in this region is about 10 times less than the corresponding ones evaluated using the data of $\langle\mu\rangle_{01}$ given by Terhune and Peters [1]. For larger E_0 field, I_1 remains approximately constant. In this respect some curious effects are worth to be noticed here. The decrease of I_1 shown by the point at $E_0 \sim 30$ kV/cm in fig. 2, right after the maximum I_1 at 20 kV/cm has been verified experimentally many times. Furthermore we have observed that once a field $E_0 > 20$ kV/cm is applied to the electrodes of the cell B for several minutes, the emitted infrared radiation I_1 fails to disappear, as expected, upon turning off the static field E_0. Upon firing the laser at regular or irregular time intervals (or even keeping the laser off for hours), I_1 decreases toward zero with a time constant that has been found roughly proportional to the field E_0 first applied to the cell and that is about 10 hours for $E_0 \sim 100$ kV/cm, We do not have yet a plausible interpretation for such a peculiar effect. We could only guess that, over a certain field threshold (that looks very sharp indeed), electrons are stripped from molecules and re-combine slowly. Their presence in the focal region could trigger a laser induced plasma which emits in the infrared, but *not* in the optical range as sparks are not detected by eye even when $E_0 = 100$ kV/cm is applied at the electrodes. Another interpretation of the effect could be an effective persistence of the static field in the focal region due to charge accumulation, or to some kind of spontaneous polarization appearing on the surfaces of the thin teflon sheets that cover the metallic electrodes. A preliminary test based on the deflection of β-particles passing between the electrodes, seems to rule out this second possibility. In any case we feel that such interesting effect is worth to be carefully investigated and we plan to do so in the near future.

The first direct measurement of the molecular vibrational coherence relaxation time T_2 of the H_2 molecule has been performed by our method[★]. As is well known this fundamental quantity presides over the all set of transient effects involving elementary excitations in material media, like photon echo [20], self induced transparency [21], transient nutation effects [22] and others [23]. In the case of a Raman active mode, as in our case, the exact knowledge of T_2 is of interest with relation to the class of transient coherent *two-photon* effects (like two-photon echo [8] etc.) which form an entirely open field of research.

The physical process underlying our measurement of T_2 is very simple. The H_2 molecules are driven in coherent vibrational motion during the interaction of the laser + Stokes pulses in cell B. The upper limit for that interaction time is 15 nsec in our experiment. After the disappearance of the driving field the infrared-active molecules keep emitting the coherent field at 2.4 μm following a decreasing exponential law which describes the dephasing process of the molecular vibrations. T_2 characterizes, by definition, that decay of coherence of the collective excitation of the medium. Our measurement gives at $p = 0.1$ atm a value $T_2 = 75 \pm 10$. nsec. We could compare this result with the inverse of the spontaneous Raman linewidth in the pressure region in which collision (homogeneous) broadening is dominant [18] by further extrapolating that information to $p = 0.1$ atm. We find a satisfactory agreement between the two data.

The inverse of the full Raman linewidth measured at $p = 10^2$ atm (and further extrapolated to 0.1 atm) is equal to 55 nsec [18]. That suggest that a substantial inhomogeneous contribution still affects the Raman linewidth at such a high pressure. We postpone a detailed discussion of the results of that experiment to a forthcoming more extended paper.[☆]

[★] The first measurement of the "longitudinal" relaxation time T_1 for hydrogen has been reported by De Martini and Ducuing [19].

[☆] The method that has led us to the measurement of T_2 is based on the first application to a Raman driven molecular system of a Transient Free-induction decay effect [24].

References

[1] R.W. Terhune and C.W. Peters, J. Mol. Spectr. 3 (1959) 138.
[2] H.L. Buijs and H.P. Gush, Can. J. Physics 49 (1971) 2367.
[3] L.I. Shiff, Quantum mechanics, (Mc. Graw Hill, N.Y. 1955) p. 267.
[4] Herzeberg, Diatomic molecules, (Van Nostrand, 1939).
[5] R.W. Terhune, P. Maker and C.M. Savage, Phys. Rev. Letters 8 (1962) 21.
[6] G. Mayer, C.R. Acad. Sciences B-t266- (1968) B247.
[7] F. De Martini, Il Nuovo Cimento, X, 51-B (1967) 16.
[8] F. De Martini, J. Ducuing and G. Hauchecorne, 1968 Quantum Electronics Conf. Proc., Miami (Fla).
[9] J.P. Coffinet, F. De Martini, Phys. Letters 22 (1969) 60; J.P. Coffinet and F. De Martini, ibidem 22 (1969) 752; F. De Martini, Phys. Rev. B, 4 (1971) 4556; F. De Martini, Phys. Letters 30A (1969) 319, ibid. 30A (1969) 547.
[10] F. De Martini. Esfahan Symp. on Fund. and Applied Laser physics, Wiley (1973).
[11] F. De Martini, G. Giuliani and E. Santamato, Optics Comm. 5 (1972) 126; F. De Martini, F. Simoni and E. Santamato, (to be published).
[12] A.D. May, V. Degen, J.C. Stryland and H.L. Welsh, Can. J. Physics 39 (1961) 1769.
[13] R.W. Minck, R.W. Terhune and W.G. Rado, App. Phys. Letters, 3 (1963) 181.
[14] P. Lallemand, P. Simova and G. Bret, Phys. Rev. Letters 17 (1966) 1239.
[15] N. Bloembergen, Nonlinear Optics (Benjamin, N.Y., 1965).
[16] P.N. Butcher, R. Loudon and T.P. Mc Lean, Proc. Phys. Soc. 85 (1965) 565.
[17] F. De Martini, J. Appl. Physics 37 (1966) 4503.
[18] E.E. Hageloncker, R.W. Minck and W.G. Rado, Phys. Rev. 154 (1957) 226.
[19] F. De Martini and J. Ducuing, Phys. Rev. Letters 17 (1966) 117
[20] I.D. Abella, N.A. Kurnit and S.R. Hartmann, Phys. Rev. 141 (1966) 391.
[21] S.L. Mac Call and E.L. Hahn, Phys. Rev. 183 (1969) 457.
[22] E.B. Treacy and A.J. De Maria, Phys. Letters 29A (1961) 369.
[23] E. Courtens, in: Laser Handbook (ed. by F.T. Arecchi and E.O. Schultz-DuBois; North Holland (1973) Publishing Company - Amsterdam), ch. E5.
[24] R.G. Brewer and R.L. Shoemaker, Phys. Rev. A6 (1972) 2001; Phys. Rev. Letters 28 (1972) 1430.

P. SOROKIN

HIGH RESOLUTION NONLINEAR SPECTROSCOPY. DICKE NARROWING AND DISPERSION OF THE THIRD-ORDER NONLINEAR SUSCEPTIBILITY OF H_2 NEAR THE $Q_{01}(1)$ VIBRATIONAL RESONANCE[☆]

F. De MARTINI, F. SIMONI and E. SANTAMATO[☆☆]
Istituto di Fisica G. Marconi, Università di Roma, Rome, Italy

Received 24 July 1973

The forward scattering process of motional narrowing in hydrogen gas has been investigated by an original method of nl spectroscopy of general application. The method has allowed a detailed study of the dispersion of the nl susceptibility $\chi^{(3)}(\omega)$ showing an unexpected behavior of $\chi^{(3)}(\omega)'$ near the $Q_{01}(1)$ molecular eigenfrequency.

1. Introduction

In two recent papers [1, 2] we have proposed and first applied to the investigation of the $Q_{01}(1)$ vibrational resonance of H_2, a new general method of high resolution nonlinear (nl) spectroscopy based on the detection of the coherent antistokes radiation created in a medium by resonant (or quasi-resonant) interaction of two monochromatic optical beams generated by tunable laser oscillators. For the first time in the field of Raman (or, more generally, nonlinear) spectroscopy (whether molecular or solid-state) the near-resonance frequency dependence of the *real* (anti-resonant) part of the third-order nl susceptibility $\chi^{(3)}(\omega)$ of the medium has been made accessible by our method, owing to the dependence of the antistokes beam intensity on the square-modulus of $\chi^{(3)}(\omega)$:

$$|\chi^{(3)}(\omega)|^2 = [\chi'(\omega)]^2 + [\chi''(\omega)]^2$$

(ref. [3]). In the present letter we report the results of an experiment which we consider as a significant extension of our preceding work. We have carefully investigated the process of Dicke (motional) narrowing [4] of the $\chi^{(3)}(\omega)$ lineshape of the $Q_{01}(1)$ resonance of hydrogen, for *forward scattering*[★]. The experimental results will be discussed on the basis of the existing theories of the narrowing process which lead us to some simple relations existing among several fundamental parameters of the gas (self-diffusion coefficient, T_2 relaxation time). Furthermore the dramatic effect of narrowing allows, by our apparatus, a detailed investigation of $\chi^{(3)}(\omega)$ in a frequency range which is substantially large compared to the linewidth of the resonance. In particular, upon scanning over the resonance, our experimental plot of $|\chi^{(3)}(\omega)|^2$ exhibits the effect of an anomalously large step-like discontinuity of the anti-resonant part of $\chi^{(3)}(\omega)$. That behavior, here reported for the first time for a molecular nl susceptibility, parallels the well known one in optical and ir atomic and solid-state spectroscopy and which refers to the optical dispersion of the medium in the linear regime [6].

2. Experimental set up

The experimental set-up is shown in fig. 1. A ruby

[☆] Work supported by G.N.S.M. - C.N.R.

[☆☆] Now at the Physics Department, University of Cosenza, Cosenza, Italy.

[★] *Backward scattering* investigation of the $Q_{01}(1)$ line of hydrogen has been reported by Lallemand et al. [5]. The works of Murray and Javan [5], and of Buijs and Gush [5] report evidence of forward scattering narrowing of the same line obtained by conventional methods of spontaneous spectroscopy. Owing to the sharpmess of the line and to the intrinsic limitations of the resolution of their apparatus, no detailed information on the minimum linewidth and on the thermodynamical conditions at which that one is measured, could be reached by their works.

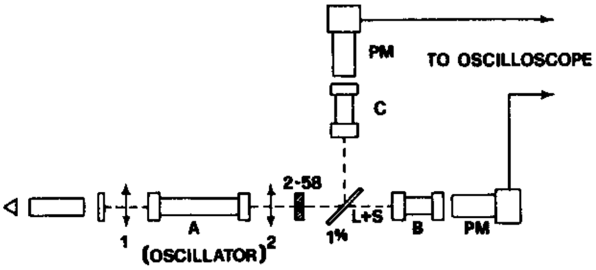

Fig. 1. Schematic diagram of the experimental apparatus.

laser, Q-switched by a rotating prism and having a mode-selector plate in place of the front mirror, was the pump of a H_2(SRS) oscillator A in which the pressure of the gas could be varied over an order of magnitude. The laser worked on a single axial mode with a linewidth $\lesssim 0.005$ cm^{-1} and the 30 nsec laser pulses had a maximum power of 5 MW. The Stokes oscillator A composed by a gas cell in which the pump beam was focused by a 15 cm $f/1$ lens, could easily be tuned over a substantial frequency range owing to the pressure-induced Raman shift effect [7]. If ω_0 is the center frequency of the $Q_{01}(1)$ resonance of H_2, that is active in SRS [8], it may be represented in terms of the gas density ρ, by the expression

$$\omega_0 = \overline{\omega}_0 + (a\rho + b\rho^2),$$

where $\overline{\omega}_0$ is the Raman shift at $\rho = 0$ and $a = -3.2 \times 10^{-3}$ cm^{-1}/amagat at $T = 300$ K. The quadratic term $b\rho^2$ is found to be negligible for $\rho \lesssim 80$ amagat [1]. As for the laser radiation, the Stokes linewidth could not be measured exactly owing to the limited finesse of our Fabry–Perot test interferometer. However, the Stokes linewidth is expected to be smaller than the laser linewidth owing to the large gain effect taking place in the (SRS) oscillator [9]. A Corning 2-58 filter cut the strong antistokes radiation generated in the cell A and the laser + stokes beams emerging from that cell at frequencies ω_ℓ and ω_S, were superimposed in the (test) H_2 cell B and in the (reference) cell C filled with nitrogen at atmospheric pressure. The antistokes signals at frequency $\omega_{AS} = (2\omega_\ell - \omega_S)$ generated in B and C owing to the 4-photon non-linear interactions, were detected by two photomultipliers. Assuming infinitely narrow lines for the laser and Stokes fields E_ℓ and E_S the non-linear source polarization at frequency ω_{AS} may be written in the simple form [4, 9]

$$P(\omega_{AS}) = \chi^{(3)}(\omega_{AS}, \omega_\ell, \omega_\ell, -\omega_S) E_\ell E_\ell E_S^*,$$

where $\chi^{(3)}$ is the third-order susceptibility of the two gases at frequency ω_{AS}. In the cell B, $\chi^{(3)}$ coincides with the complex Raman susceptibility of H_2:

$$\chi(\omega) = \chi'(\omega) + i\chi''(\omega),$$

which is resonant at the difference frequency $\omega = \omega_\ell - \omega_S$, while in the cell C, $\chi^{(3)} \equiv \overline{\chi}'$ is the non-resonant nl susceptibility of the nitrogen gas that, at frequency ω_{AS}, may be taken as a frequency-independent real quantity [10]. If the Raman gain in B is much smaller than the inverse of the characteristic interaction length of the parametric non-linear process, as in our case, the antistokes fields emerging from B and C may be taken proportional to the respective nl polarizations at frequency ω_{AS} [3, 11]. In our experiment the corresponding antistokes intensity

$$I_B(\omega)/I_C = |\chi(\omega)|^2/(\overline{\chi}')^2$$

is plotted vs the difference frequency $\omega = \omega_\ell - \omega_S$ upon sweeping over the quoted resonance of hydrogen. We shall discuss separately the two sets of physical information that could be drawn from our results: the one corresponding to the Dicke narrowing itself and the jump of nl molecular polarizability.

3. Dicke narrowing

The plot reported in fig. 2 shows the effect of motional narrowing of the $Q_{01}(1)$ resonance of hydrogen at $T = 300$ K for forward scattering. The values of the linewidths of $\chi''(\omega)$ were evaluated on the basis of our

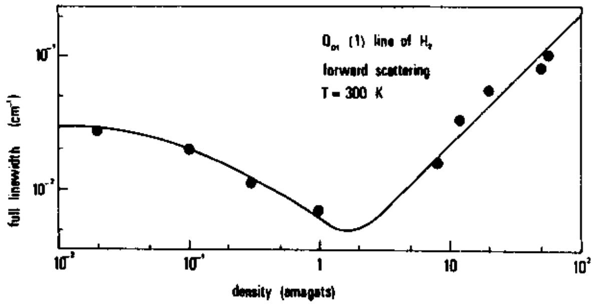

Fig. 2. Plot of the full linewidths of the $Q_{01}(1)$ resonance of H_2, vs. gas density.

experimental data on $|\chi^{(3)}(\omega)|^2$ assuming a lorentzian-line model for gas densities ranging from 2×10^{-1} amagats upwards. For lower densities where Doppler (inhomogeneous) broadening is dominant a gaussian shape model was assumed [12]. A justification for assuming the lorentzian model in the Dicke narrowing region is given by the following theoretical considerations. An expression of $\chi''(\omega)$ may be obtained by Fourier transforming the autocorrelation function $F(\tau)$ of the scattered field. The general expression for $F(\tau)$ may be given in the following form [13]:

$$F(\tau) = \lim_{T\to\infty} \int_{-T}^{+T} \exp\{-\mathrm{i}[\Delta\varphi(t,\tau) + 2\pi\lambda^{-1}\Delta x(t,\tau)]\}\,\mathrm{d}t,$$

where $\Delta\varphi(t,\tau) = [\varphi(t+\tau) - \varphi(t)]$ is the phase perturbation due to a collision, $\Delta x(t,\tau) = [x(t+\tau) - x(t)]$ represents the motion accounting for the Doppler effect and λ is written, for forward scattering kinematics in terms of laser and stokes wavelengths as

$$\lambda = \lambda_S\lambda_\ell/(\lambda_S - \lambda_\ell).$$

By making the hypothesis of no statistical correlation between the ensembles $\{\Delta x\}$ and $\{\Delta\varphi\}$ the phase autocorrelation function may be given in the form [13, 14]:

$$F'(\tau) = \exp\{-(\tau/\tau_\ell)[(1-A) + \mathrm{i}B]\},$$

where τ_ℓ is the mean free time among the Poisson distributed collisions *which disturb the phase* and

$$A + \mathrm{i}B \equiv \int_0^{2\pi} \exp(\mathrm{i}\Delta\varphi)\,p(\Delta\varphi)\,\mathrm{d}(\Delta\varphi),$$

being $p(\Delta\varphi)$ the probability density function of the phase disturbances. The factor $(1-A)/\tau_\ell$ accounts for pressure broadening (collision limited lifetime) while B is responsible for a (small) line shift, as shown later. Breene [15] and Galatry [13] have evaluated the expression of the autocorrelation function $F''(\tau)$ corresponding to the molecular motion by making use of the maxwellian distribution for the set of velocities v_0 and by assuming for the set of variables $\{\Delta x(t,\tau)\}$ the generalized "diffusion" probability function due to Chandrasekhar [16]:

$$W(\Delta x/v_0, \tau) = \sqrt{\bar{A}/\tau} \times \exp\{-\bar{A}[\Delta x - v_0(1-\exp(-\beta\tau))/\beta]^2\},$$

where

$$\bar{A} \equiv m\beta^2/(2kT)\cdot\{2\beta\tau - 3 + 4\exp(-\beta\tau) - \exp(-2\beta\tau)\},$$

β is the coefficient of dynamical friction of the gas:

$$\beta \equiv kT/mD \sim 1/\tau_D$$

and τ_D is the mean free time among collisions. The final expression of $F''(\tau)$ may be evaluated in closed form [15] and, for a gas of equal molecules with mass m, is given by:

$$F''(\tau) = \exp\left\{-\frac{4\pi^2 kT}{m\beta^2\lambda^2}\cdot[\beta\tau - 1 + \exp(-\beta\tau)]\right\}.$$

We verify that, setting $\beta\tau \leqslant 1$ in $F''(\tau)$ and expanding to second order the exponential in curly brackets, we get the Fourier transform of the Doppler lineshape

$$F''(\tau) \sim \exp\left[-\frac{2\pi^2 kT}{m\lambda^2}\tau^2\right]$$

which is independent of D. We may now Fourier transform the overall correlation function

$$F(\tau) = F'(\tau)F''(\tau)$$

and obtain the final expression of $\chi''(\omega)$:

$$\chi''(\omega) = \chi''(\omega_0) \times \frac{[(1-A)/\tau_\ell + 4\pi^2 D/\lambda^2]^2}{[\omega - \omega_0 - B/\tau_\ell]^2 + [(1-A)/\tau_\ell + 4\pi^2 D/\lambda^2]^2}. \tag{1}$$

We may neglect the effect of B which is very small and could not be detected in our experiments.

Expression (1) may be taken as the basis of the interpretation of our results. Recalling the inverse dependence of D and $T_2 \sim \tau_\ell/(1-A)$ on the gas density (i.e. pressure) [17] we may easily verify that maximum narrowing corresponds to

$$(1-A)/\tau_\ell = 4\pi^2 D/\lambda^2.$$

Furthermore the minimum value of the linewidth $\Delta\omega$ is related to the Doppler width $\Delta\omega_D$ by the simple expression:

$$\Delta\omega = \sqrt{2/\ln 2}\,\Delta\omega_D\sqrt{\alpha},$$

being $\alpha = \tau_D(1-A)/\tau_\ell \leqslant 1$ the fraction of collisions which are active in dephasing the field. Dicke narrowing is present only for $\alpha < 1$, i.e. for resonances which are somewhat highly "screened" against "hard" collisions, as, for electric dipole transitions, for some totally symmetric Raman modes. We may try to apply the simple equations we have just obtained to the case of hydrogen using the experimental results shown in fig. 2. If we assume for hydrogen the value of the self-diffusion coefficient calculated from Loschmidt's experiment [17] $D = 1.31$ ($T = 15°\mathrm{C}, p = 1$ atm), we get a value of $\tau_\ell/(1-A) = 1.79$ nsec at $\rho = 1.68$ ama, corresponding to the minimum linewidth. That value is only in a order-of-magnitude agreement with the value of T_2 evaluated by making use of the values of the linewidth at high pressures (where collision broadening is dominant) taking further into account the pressure dependence of T_2. Using for instance our data at the gas density of 10^2 amagats: $\Delta\nu_\mathrm{f} \simeq 2 \times 10^{-1}\ \mathrm{cm}^{-1}$ we get at $\rho = 1.68$ ama a value $T_2 = 3.15$ nsec. On the grounds of the results of a recent direct measurement of T_2 in hydrogen performed in our laboratory [18] we may say that the factor two discrepancy we have found between the two relaxation times cannot be explained invoking for hydrogen possible inhomogeneous contributions to the high pressure linewidths, which are small. We may rather say that the theoretical approach we have adopted needs modifications for such a very light molecule as H_2 [19]. We postpone a detailed discussion on this point to a next more extended paper. Proceeding further on our discussion it seems to be interesting to evaluate, on the basis of the ratio between the experimental values of the Dicke and Doppler linewidths, the fraction α of collisions which are active in dephasing the molecular vibration. Using the expression we have given above we find for hydrogen $\alpha = 0.96\%$.

4. Spectral analysis of $|\chi^{(3)}(\omega)|^2$

The general expression of the third-order optical susceptibility for a molecular gas has been worked out by several authors and may be found in [3] and [20]. It consists of the sum of 24 terms which are in turn proportional to the triple sum over the intermediate states of the electric dipole matrix elements $\langle\mu\rangle$ connecting the ground state (the only one which we suppose to be appreciably populated) to the set of the other molecular resonances. The usual approximation that is made in case of Raman effect, when the effect of a single resonance is dominant, is to pick out, from these addenda, the only two ones that exhibit a resonant behavior at the corresponding eigenfrequency. When this approximation is made, considering the case of antistokes scattering the general expression of $\chi^{(3)}$ reduces to the form

$$\chi^{(3)}_{\mu\alpha\alpha\beta}(\omega_\ell, \omega_\ell, -\omega_\mathrm{S})$$

$$= \frac{\rho_\mathrm{ii}(0) - \rho_\mathrm{ff}(0)}{\hbar\{[\omega_\mathrm{fi} - (\omega_\ell - \omega_\mathrm{S})] + \mathrm{i}\Gamma} A^{\alpha\beta}_\mathrm{fi}(\omega_\ell) A^{\mu\alpha *}_\mathrm{fi}(\omega_\mathrm{AS}),$$

where μ, α and β are labels for the polarization components of the ω_AS, ω_ℓ, ω_S beams and $A^{\alpha\beta}_\mathrm{fi}(\omega)$ are non resonant terms:

$$A^{\gamma\delta}_\mathrm{fi} = \frac{1}{\hbar} \sum_t \left[\frac{\langle \mathrm{f}|\mu_\gamma|t\rangle\langle t|\mu_\delta|\mathrm{i}\rangle}{\omega_{t\mathrm{f}} + \omega_\ell} + \frac{\langle \mathrm{f}|\mu_\delta|t\rangle\langle t|\mu_\gamma|\mathrm{i}\rangle}{\omega_{t\mathrm{i}} - \omega_\ell} \right].$$

If we want now to evaluate the frequency dependence of the real and imaginary parts of $\chi^{(3)}(\omega)$ in the vicinity of the $Q_{01}(1)$ resonance ($\omega_0 = 4155.21\ \mathrm{cm}^{-1}$) for normal hydrogen, we should not overlook the contributions of the nearby vibro-rotational lines corresponding to different values of J:

$Q_{01}(0)$ ($\omega_0 = 4161.08\ \mathrm{cm}^{-1}$),
$Q_{01}(2)$ ($\omega_0 = 4143.43\ \mathrm{cm}^{-1}$),
$Q_{01}(3)$ ($\omega_0 = 4125.82\ \mathrm{cm}^{-1}$)

which, for the natural mixture of ortho- and para-hydrogen, as in our case, may contribute to the nl optical dispersion.

In fig. 3 the theoretical plots of $\chi^{(3)\prime}(\omega)$ and $\chi^{(3)\prime\prime}(\omega)$ for $\omega_0 = 4155.21\ \mathrm{cm}^{-1}, p = 1$ atm, $T = 300$ K, are drawn assuming a lorentzian lineshape taking further into account the effect of the $J = 0, 2, 3$ rotational resonances with their respective intensities, for normal hydrogen [21]. The corresponding theoretical plot of $|\chi^{(3)}(\omega)|^2$ is also displayed in fig. 3.

The behavior of the experimental curve of $|\chi^{(3)}(\omega)|^2$ also shown in fig. 3 is, in some respect, unexpected and somwhat puzzling. The step-like jump shown by $|\chi^{(3)}(\omega)|^2$ upon sweeping over the resonance may be thought to correspond to the contribution of the strong $Q_{01}(1)$ resonance to the dispersion of the Raman polarizability, a behavior well known in linear optics [6] and here reported for the first time for a nl, Raman,

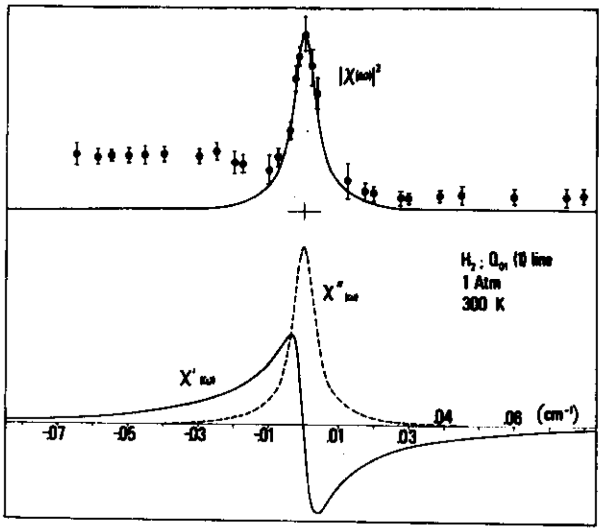

Fig. 3. Frequency dependence of the $\chi^{(3)'}(\omega)$, $\chi^{(3)''}(\omega)$ and $|\chi^{(3)}(\omega)|^2$ functions in the vicinity of the $Q_{01}(1)$ resonance of H_2 at $\omega_0 = 4155.21$ cm^{-1}. The theoretical curves are evaluated taking into account the effect of the $Q_{01}(0)$, $Q_{01}(2)$, $Q_{01}(3)$ vibro-rotational resonances. The scales of the experimental and theoretical $|\chi^{(3)}|^2$ plots are arbitrary. The superposition of the two curves is determined by the coincidence at the top of the peaks, at $\omega = \omega_0$.

process. In addition the plateau shown by $|\chi^{(3)}(\omega)|^2$ for $\omega > \omega_0$ may well be attributed to the effect of the nonresonant contribution to $\chi^{(3)'}(\omega) : \chi'_{nl}(\omega)$. The only unexpected effect is that the size of these out-of-resonance contributions to $\chi^{(3)'}(\omega)$ compared with the height of the peak at $\omega = \omega_0$ is about three orders of magnitude larger than expected. At that point some experimental details are worth to be discussed in order to rule out possible misinterpretations of our results: a) In the test cell B the driving laser and Stokes pulses had about 10 kW of power focused by a 15 cm $f/1$ lens in a focal interaction region $l \simeq 3$ cm. That value of l may be compared with the coherence length l_c for the antistokes interaction process which has been evaluated to be $l_c \simeq 80$ cm for hydrogen at $p = 1$ atm. In addition the resonant (SRS) gain in the same conditions is [9] $g \simeq 5 \times 10^{-2}$ cm^{-1}. Thus exponential growth effects in the test cell are strictly negligible [11]. b) Molecular saturation effects at resonance are found to be also negligible. We have checked that at $\omega = \omega_0$, by varying the laser and Stokes intensities I_ℓ, I_S over an order of magnitude, the antistokes intensity keeps rigorously proportional to $I_\ell^2 I_S$, as expected [3]. c) The intensity of the antistokes peak at $\omega = \omega_0$, compared with the intensity of the reference beam emerging from the cell c) corresponds to an absolute value of $\chi^{(3)''}(\omega_0)$ for H_2 which agrees with the absolute value of the nonresonant $\bar{\chi}^{(3)'}$ of the reference gas (N_2) first measured by Rado [10]. We may rather add, in this connection, that $\bar{\chi}^{(3)'}$ for various gases have in turn been measured by our apparatus, in the test cell C, by comparison with the resonant value of $\chi^{(3)''}(\omega_0)$ for H_2. They are reported in table 1. The results for N_2, O_2 agree within 5% with the data [10]. Our result for He is about 4 times larger than the one reported in [10]. d) The dramatic jump of $\chi^{(3)'}(\omega)$ polarizability of H_2 near the $Q_{01}(1)$ resonance, we have found in the present experiment, may well explain the substantial distortion of the $|\chi^{(3)}(\omega)|^2$ line at $p = 20$ atm we have reported in ref. [1].

Table 1

	$\chi_{NR}^{(3)'} \times 10^{18}$ cm^3/erg
N_2	1.35
O_2	1.26
He	0.37
air	1.30

5. Conclusions

In conclusion we believe that our present results strongly suggest the existence of some very interesting processes affecting the lineshapes $\chi^{(3)'}(\omega)$ and $\chi^{(3)''}(\omega)$ in the motional narrowing region, in hydrogen gas. As fas as the experiment is concerned we plan to pursue our spectroscopic work in H_2 and other gases by extending the spectral range of our high resolution apparatus by using other kinds of tunable lasers.

Acknowledgement

We acknowledge useful discussions and substantial help received from dr. G. Giuliani and D. Di Bucchianico.

References

[1] F. De Martini, in Esfahan Symposium on laser physics; Wiley (1973).
[2] F. De Martini, G.P. Giuliani and E. Santamato, Optics Comm., 5 (1972) 126.
[3] N. Bloembergen, Nonlinear optics (Benjamin, N.Y. 1965).
[4] R.H. Dicke, Phys. Rev. 89 (1973) 472;
J.P. Wittke and R.H. Dicke, Phys. Rev. 103 (1956) 620.
[5] P. Lallemand, P. Simova and G. Bret, Phys. Rev. Letters 17 (1966) 1239;
J. Murray and A. Javan, J. Hol. Spectroscopy 29 (1969) 502;
H.L. Buijs and H.P. Gush, Can J. Physics 49 (1971) 2366.
[6] C. Kittel, Introduction to solid-state physics (II Ed. Wiley, 1953), p. 165.
[7] A.D. May, V. Degen, J.C. Stryland and H.L. Welsh, Can. J. Physics 39 (1961) 1769.
[8] R.W. Minck, R.W. Terhune and W.G. Rado, Appl. Phys. Lett. 3 (1963) 181.
[9] J. Ducuing in: Glauber, Quantum Optics (Academic Press, N.Y., 1970).
[10] W.G. Rado, Appl. Phys. Letters 11 (1967) 123.
[11] F. De Martini, Il Nuovo Cimento 51 B (1967) 16.
[12] G.E. Pake and E.M. Purcell, Phys. Rev. 74 (1948) 1184.
[13] L. Galatry, Phys. Rev. 122 (1961) 1218.
[14] M. Magenau and M.B. Lewis, Rev. Mod. Physics 31 (1959) 569.
[15] R.G. Breene, Rev. Mod. Physics, 29 (1957) 94.
[16] S. Chandraseckhar, Rev. Mod. Phys. 15 (1943) 1.
[17] J. Jeans, Kinetic theory of gases (Cambridge Un. Press London p. 214 (1962).
[18] F. Capasso and F. De Martini (to be published).
[19] A.D. May, private communication to F.D.M.;
V.I. Alekseev and I.I. Sobel'man, Sov. Phys. JETP 28 (1969) 991;
J.I. Gersten and H.M. Foley, J. Opt. Soc. Am. 58 (1968) 933.
[20] P.N. Butcher, Nonlinear Optical phenomena, Bull. 200 Ohio State University, Columbus 1965 (p. 98).
[21] A.D. May, G. Varghese, J.C. Stryland and H.L. Welsh, Can. J. Physics 42 (1964) 1058.

Nonlinear Spectroscopy of Bulk and Surface Polaritons (*).

F. De Martini

Istituto di Fisica dell'Università - 00185 *Roma, Italia*

1. – Introduction.

In recent years the advent of mode-locked and narrow-band frequency-tunable lasers has made possible a new kind of investigation in solid-state spectroscopy: the coherent excitation of elementary excitations of various kinds by resonant interaction with laser fields via a linear or nonlinear mechanism. Obviously, the fundamental laws of nonlinear optics, as they are presented in ref. [1], apply to the new situation, but they should be complemented by a new class of theories. Processes like resonant fluorescence, transient coherent propagation phenomena like self-induced transparency, local coherence effects like photon-echo and optical nutation, and some aspects of the propagation of polariton fields in solids often require new theoretical approaches leading to problems that are sometimes unsolvable with present techniques of mathematical physics. However, in crystalline solids the coherence relaxation time T_2 of most of the elementary excitations is generally so short with respect to the amount of energy that can be stored in a laser pulse without damage to the medium, that transient coherence effect can hardly be detected. Therefore, we limit ourselves in these lectures to considering some simple aspects of the theory of the polariton field generation and propagation, starting from conventional classical electrodynamics and quantum mechanics. In view of recent nonlinear experiments involving bulk polaritons, some of which are being presented at the present school, we devote our attention to only few effects, namely to nonlinear mixing processes such as sum frequency generation (SFG), difference frequency generation (DFG), and to coherent-scattering processes like those involved in the experiments of 4-photon coherent spectroscopy. We shall first outline a linear transient propagation theory of the fields in SFG and DFG and obtain the expression for parametric gain valid in either case.

(*) Work supported by Gruppo di Ricerca Elettronica Quantistica e Plasmi of the C.N.R. and by NATO 1155 joint program between Università di Roma and University of California at Berkeley.

We conclude with a brief presentation of the most relevant experiments that have been carried out recently in the field, including some of the author's own results. We shall present, at the end of the paper, the first formulated theory of the nonlinear excitation of the surface polaritons and the results of the first experiment on 4-photon excitation of surface polaritons in GaP.

2. – Transient propagation theory of the bulk polariton sum and difference frequency generation.

The parametric sum and difference frequency generation processes involving the scattering of a coherent polariton wave may be described by starting either from the classical coupled-wave theory, largely used in nonlinear optics [1], or from a quantum transition rate formulation [2]. The theory of the gain affecting the « signal » (optical) wave in a parametric process, in which the frequency of one of the interacting fields is near a lattice resonance, has been considered by SHEN [3], BUTCHER and MCLEAN [4] and by HENRY and GARRETT [5], according to the classical approach. The application of the classical method, which is usually concerned with e.m. fields rather than with energy flow, becomes difficult when a complete description of the dynamics of a three-wave interaction is required. In order to overcome serious mathematical problems, some approximations are usually introduced in the theory, for example the lack of the depletion of the pump and the *a priori* hypothesis of a single exponential gain solution for the waves in the case of the difference frequency generation. As we shall see below, these approximations are indeed not appropriate to a transient analysis involving polariton particles rather than photons.

As long as we limit ourselves to considering a negligible change of population of the exciton state, the interacting e.m. and polariton fields may be expressed in terms of boson creation and annihilation operators, which satisfy the commutation relations

$$[b_{k_i}, b^\dagger_{k_j}] = \delta_{k_i k_j} \qquad (i, j = 1, 2, 3). \tag{1}$$

If m_{k_1}, m_{k_2}, m_{k_3} are the mode occupation numbers for the three fields, the matrix elements of these operators in the Fock space are

$$\begin{cases} \langle m_{k_i} - 1 | b_{k_j} | m_{k_j} \rangle = m^{\frac12}_{k_i}\, \delta_{k_i k_j}\,, \\ \langle m_{k_i} + 1 | b^\dagger_{k_j} | m_{k_j} \rangle = (m_{k_i} + 1)^{\frac12}\, \delta_{k_i k_j}\,. \end{cases} \tag{2}$$

In the above expressions the symbols k_i represent the momenta of the fields $\boldsymbol{E}_i$.

The fields, assumed to be monochromatic plane waves, may be written in the following form [6]:

$$\begin{cases} \boldsymbol{E}_1(\omega_1) = \left(\dfrac{h\omega_1^3}{k_1^2 c^2 V}\right)^{\frac12} \boldsymbol{p}_1(b_{k_1} \exp[i\boldsymbol{k}_1\cdot\boldsymbol{r}] + b^\dagger_{k_1} \exp[-i\boldsymbol{k}_1\cdot\boldsymbol{r}])\,, \\ \boldsymbol{E}_2(\omega_2) = \left(\dfrac{h\omega_2^3}{k_2^2 c^2 V}\right)^{\frac12} \boldsymbol{p}_2(b_{k_2} \exp[i\boldsymbol{k}_2\cdot\boldsymbol{r}] + b^\dagger_{k_2} \exp[-i\boldsymbol{k}_2\cdot\boldsymbol{r}])\,, \\ \boldsymbol{E}_q(\omega_3) = \left(\dfrac{h\omega_3 v_p v_g}{c^2 V}\right)^{\frac12} \boldsymbol{p}(b_{k_3} \exp[i\boldsymbol{k}_3\cdot\boldsymbol{r}] + b^\dagger_{k_3} \exp[-i\boldsymbol{k}_3\cdot\boldsymbol{r}])\,, \\ \boldsymbol{Q}(\omega_3) \;= (4\pi N\mu\omega_0^2)^{-\frac12}\cdot(c^2/v_p v_g - \varepsilon_\infty)^{\frac12}\boldsymbol{E}_q(\omega_3)\,. \end{cases} \tag{3}$$

In the above expressions V is a volume of the solid with linear dimensions small compared to the inverse of the absorption coefficient $\alpha(\omega_3)$; N is the volume density of the primitive cells of the crystal; v_p and v_g are, respectively, the phase and the group (energy) velocity of the undamped polariton wave; μ is the reduced mass of the ionic or electronic oscillator relative to one primitive cell of the crystal and associated with the TO lattice mode at frequency $\omega_{\text{TO}} \equiv \omega_0$ or, correspondingly, with the TO excitonic mode. ε_∞ is the high-frequency dielectric constant and the expressions of $v_p(\omega_3)$ and $v_g(\omega_3)$ may be obtained by the classical Huang dispersion theory [7] or by its quantum-mechanical counterpart [8]. If we allow for a phase mismatch of the waves, $\Delta\boldsymbol{k} = \boldsymbol{k}_1 \pm \boldsymbol{k}_2 - \boldsymbol{k}'_3$ $(\boldsymbol{k}_3 = \boldsymbol{k}'_3 + i\boldsymbol{k}''_3)$, an interaction Hamiltonian density for the coupled-field system may be expressed in the following form (*):

$$\mathscr{H} = A\boldsymbol{p}_1\boldsymbol{p}_2\boldsymbol{p} \,\vdots\, \underline{d}(b_1 b_2^\dagger b_3^\dagger \exp[i\Delta\boldsymbol{k}\cdot\boldsymbol{r}] + b_1^\dagger b_2 b_3 \exp[-i\Delta\boldsymbol{k}\cdot\boldsymbol{r}]) \tag{4}$$

for DFG and

$$\mathscr{H} = A\boldsymbol{p}_1\boldsymbol{p}_2\boldsymbol{p}_3 \,\vdots\, \underline{d}(b_1 b_2 b_3^\dagger \exp[i\Delta\boldsymbol{k}\cdot\boldsymbol{r}] + b_1^\dagger b_2^\dagger b_3 \exp[-i\Delta\boldsymbol{k}\cdot\boldsymbol{r}]) \tag{4'}$$

for SFG. A is a constant to be determined on the basis of the coefficients of the fields of (3) and $\underline{d}$ is the nonlinear susceptibility tensor that accounts for the coupling. A significant expression for the nonzero elements of $\underline{d}$ near the TO resonance has been given by FAUST and HENRY [9] in the form $\underline{d} = \underline{d}_E(1 + C\omega_0^2 D^{-1})$, where $C = e^* N\underline{d}_Q/\mu\omega_0^2\underline{d}_E$ is a tensor parameter that characterizes the nonlinear response of the crystal, e^* is the effective charge of the oscillators and $D = \omega_0^2(k_3) - \omega^2 - i\omega\Gamma$, Γ being the damping parameter of the oscillator.

(*) The upper sign appearing in the expression of $\Delta\boldsymbol{k}$ corresponds to SFG. Hereafter in the paper we shall adopt this convention.

The interaction Hamiltonian H_1 is found by integrating $\mathscr{H}$ over the volume V. If we consider one initial state $|m_{k_1}, m_{k_2}, m_{k_3}\rangle$ for the fields, then the transition probability, over a unit frequency range per unit time corresponding to the scattering of a pump photon, is given by the following expression [10]:

$$(5)\qquad w = \frac{4\pi^2}{\hbar^2}\big(|\langle m_{k_1}-1, m_{k_2}\mp 1, m_{k_3}+1|H_1|m_{k_1}, m_{k_2}, m_{k_3}\rangle|^2 - \\ -|\langle m_{k_1}+1, m_{k_2}\pm 1, m_{k_3}-1|H_1|m_{k_1}, m_{k_2}, m_{k_3}\rangle|^2\big)\frac{\frac{1}{2}\alpha(\omega_3)}{|\Delta \boldsymbol{k}|^2+[\frac{1}{2}\alpha(\omega_3)]^2}\,\delta(\Delta\omega)\,,$$

where $\Delta\omega = \omega_1 \pm \omega_2 - \omega_3$, and $\alpha(\omega_3) = 2|\boldsymbol{k}_3''(\omega_3)|$ is the absorption coefficient. The Lorentzian factor depending on $\Delta \boldsymbol{k}$ in eq. (5) accounts for the damping of the final polariton momentum state that is characterized by the absorption coefficient α. The damping affecting the final-energy state of the interaction is characterized by a frequency-dependent damping parameter $\Gamma(\omega_3)$ that is related to $\alpha(\omega_3)$ through the polariton group velocity:

$$(6)\qquad \Gamma(\omega_3) = v_g(\omega_3)\,\alpha(\omega_3)\,.$$

If we make use of eq. (2), w becomes

$$(7a)\qquad w = \frac{B}{V}\,\frac{(\frac{1}{2}\alpha)^2}{|\Delta \boldsymbol{k}|^2+(\frac{1}{2}\alpha)^2}\,\delta(\Delta\omega)\cdot[\;]\,,$$

where

$$[\;] \equiv [m_{k_1}m_{k_2} - m_{k_3}(m_{k_1}+m_{k_2}+1)] \qquad \text{(SFG)}\,,$$

$$[\;] \equiv [m_{k_1}(m_{k_2}+m_{k_3}+1) - m_{k_2}m_{k_3}] \qquad \text{(DFG)}$$

and

$$(7b)\qquad B = \frac{32\pi^5\hbar\omega_1^3\omega_2^3\omega_3^3 v_g v_0 |d|^2}{|\boldsymbol{k}_1|^2|\boldsymbol{k}_2|^2c^6}\,.$$

In view of the discussion of our experiment dealing with a cubic crystal (GaP) belonging to the $\bar{4}3m$ class, we have omitted in (7b) the tensor notation for the nonlinear coupling coefficient d. Hereafter we shall consider d, d_E, d_Q as scalar quantities, because, for the given symmetry and crystal class, these tensors are determined by only one parameter [11].

By integrating eq. (7a) over the distribution of the final-energy states, we obtain the transition probability per unit time

$$(8)\qquad W = \frac{B}{\pi^2 v_g V}\,\frac{(\frac{1}{2}\Gamma)^2}{(\Delta\omega)^2+(\frac{1}{2}\Gamma)^2}\,\frac{(\frac{1}{2}\alpha)^2}{|\Delta \boldsymbol{k}|^2+(\frac{1}{2}\alpha)^2}\times[\;]\,.$$

Equation (8) is valid when $\Delta\omega$ and $|\Delta \boldsymbol{k}|$ are not too much larger than the corresponding damping parameters Γ and α.

As will be shown, the polariton density is much smaller than the photon densities at frequencies ω_1 and ω_2. Hence for $m_{k_3} \gg 1$ we can write a simplified expression of W in the form

$$(9a)\qquad W = \frac{g\,m_{k_1}m_{k_2}}{V}\,,$$

where

$$(9b)\qquad g \equiv \frac{B}{\pi^2 v_g}\,\frac{(\frac{1}{2}\alpha)^2}{|\Delta \boldsymbol{k}|^2+(\frac{1}{2}\alpha)^2}\,\frac{(\frac{1}{2}\Gamma)^2}{(\Delta\omega)^2+(\frac{1}{2}\Gamma)^2}\,.$$

We consider in this section a collinear interaction of the fields along the direction z normal to the entrance face of the crystal. The fields are written as functions of the corresponding z-co-ordinate, which is positive in the crystal and zero at the surface.

In this section we also consider a phase-matched interaction. The equation describing the evolution of the densities of the pump photons $\varrho_1(z, t) \equiv m_{k_1}/V$ and $\varrho_2(z, t) \equiv m_{k_2}/V$ may be written, owing to (9), in the following form:

$$(10)\qquad \frac{\partial \varrho_2}{\partial t} + v_2\frac{\partial \varrho_2}{\partial z} = \pm\left(\frac{\partial \varrho_1}{\partial t} + v_1\frac{\partial \varrho_1}{\partial z}\right) = \mp g\varrho_1\varrho_2\,,$$

where v_1 and v_2 are the group velocities of the two waves. For negligible optical dispersion of the medium at the frequencies ω_1 and ω_2 we have $v_1 = c/n_1$ and $v_2 = c/n_2$, where n_1 and n_2 are the refractive indices. Our present theory is greatly simplified if we set $v_1 = v_2$ in eq. (10).

We can now write the fields as functions of the propagation variables:

$$(11)\qquad w_1 = t + z/v_1\,,\qquad \bar{w}_1 = t - z/v_1\,.$$

The corresponding inverse relations are $t = \frac{1}{2}(w_1 + \bar{w}_1)$ and $z = (w_1 - \bar{w}_1)\frac{1}{2}v_1$. A first integral of (10) is given by the following expression:

$$(12)\qquad \varrho_1(w_1, \bar{w}_1) \mp \varrho_2(w_1, \bar{w}_1) = f(\bar{w}_1)\,.$$

The difference (sum) of the pump photon wave packets is a forward-propagation arbitrary function. We impose the following boundary condition on the solution. At $z = 0$, $w_1 = \bar{w}_1$, the ratio of the two fields is a prescribed function of time, $\varrho_1(0, t)/\varrho_2(0, t) = \varepsilon(t)$. We rewrite that condition in the notation of the propagating frame, eq. (11), and we make use of eq. (12) in order to write the driving term $\varrho_1\varrho_2$ appearing in eq. (10) as a function of one of the fields. The solution of (10) is now straightforward. By restoring the initial variables but still keeping the useful notation $\overline{w}_1 = t - z/v_1$, the product of the fields is found to be

$$\text{(13)}\qquad \begin{cases} \varrho_1 \varrho_2 = [\tfrac{1}{2} f(\overline{w}_1)]^2 \operatorname{cosech}^2 \{G_1 f(\overline{w}_1)(z - \bar{z}(\overline{w}_1))\} & \text{(SFG)},\\ \varrho_1 \varrho_2 = [\tfrac{1}{2} f(\overline{w}_1)]^2 \operatorname{sech}^2 \{G_1 f(\overline{w}_1)(z - \bar{z}(\overline{w}_1))\} & \text{(DFG)}. \end{cases}$$

In the above expressions we have introduced the parameter $G_1 \equiv g/4v_1$ and the function $\bar{z}(\overline{w}_1) \equiv \mp [\ln \varepsilon(\overline{w}_1)]/[2G_1 f(\overline{w}_1)]$ that accounts for the initial conditions. Note that $\bar{z}$ is always negative for SFG. A simple equation relates the two fields:

$$\text{(14)}\qquad \varrho_2(z, t) = \varrho_1(z, t) \exp[\mp 2G_1 f(\overline{w}_1)(z - \bar{z}(\overline{w}_1))],$$

which, in the case of DFG, accounts for the stimulated-scattering exponential growth.

The continuity equation for the polariton density $\varrho_q(z, t) = m_{k_q}/V$ is given in the following form:

$$\text{(15)}\qquad \frac{\partial \varrho_q}{\partial t} + v_q \frac{\partial \varrho_q}{\partial z} = g(\omega_3)\varrho_1\varrho_2 - \Gamma'(\omega_3)\varrho_q,$$

where $\Gamma'(\omega_3)$ is a phenomenological «damping» parameter that accounts for the relaxation of the polaritons to the ground state. Making use of the notation of magnetic resonance [12], we can associate $\Gamma'(\omega_3)$ with the longitudinal relaxation time T_1, and write $\Gamma'(\omega_0) = 1/T_1$. We notice that, in general, $\Gamma'(\omega_0) \equiv \Gamma'$ is smaller than the parameter $\Gamma(\omega_0) \equiv \Gamma$ that appears in the expression for $g(\omega_0)$ given by eq. (9*b*). In effect, $\Gamma(\omega_0)$ is the line width of the polariton resonance and is determined, competitively, by the inhomogeneous broadening process and by the effect of the coherence relaxation. When this last effect is overwhelming, the line width of the TO resonance $\Gamma \equiv \Gamma(\omega_0)$ is approximately equal to the inverse of the transverse relaxation time T_2. Obviously the present considerations on the effects of the different homogeneous broadening processes are physically relevant only when we are dealing with quantum systems that are not too strongly coupled by collisions, *e.g.* excited molecules in a gas. In that case $T_2 \ll T_1$. For optical phonons in solids at normal temperature we can assume $T_1 \simeq T_2$.

In the present section we shall consider a driving pulse $f(\overline{w}_1)$ that is a regular analytic function of $\overline{w}_1$. With no loss of generality and for simplicity's sake, we shall mainly deal with a symmetric pulse characterized by a time duration $\Delta\tau = (k')^{-1}$, that is approximately equal to the inverse of the time derivative of $f(\overline{w}_1)$, *e.g.* $f(\overline{w}_1) = \operatorname{sech}(k'\overline{w}_1)$.

In order to solve eq. (15), we again apply a transformation of variables from the set $\{z, t\}$ to the propagation set $\{w, \overline{w}\}$, where $w = t + z/v_q$ and $\overline{w} = t - z/v_q$. The functions $f(\overline{w}_1)$ and $\bar{z}(\overline{w}_1)$ appearing in eq. (13) are now written in terms of the new variables according to the equation $\overline{w}_1 = \tilde{\alpha}w + \tilde{\delta}\overline{w}$, with $\tilde{\alpha} \equiv (1 - \tilde{\beta})/2$, $\tilde{\delta} \equiv (1 + \tilde{\beta})/2$ and $\tilde{\beta} \equiv v_q/v_1 \ll 1$.

In the new frame, eq. (15) is a standard linear equation whose general solution may be expressed in the following integral form:

$$\text{(16)}\qquad \varrho_q(w, \overline{w}) = \exp[-\Gamma' w/2]\left[C_2(\overline{w}) + (g/2)\int \varrho_1 \varrho_2 \exp[\Gamma' w/2]\,\mathrm{d}w\right],$$

where $C_2(\overline{w})$ is an arbitrary function of $\overline{w}$, to be determined by the boundary conditions.

The integral appearing in (16) may be calculated in successive integrations by parts, taking at each step the exponential function as the differential factor of the integration. For $\Gamma' \gg k'$ and $g\tilde{\beta} \ll \Gamma'$ we obtain in this way a rapidly converging series with terms proportional to increasing powers of k'/Γ'. As the minimum line width of the polariton resonance in solids is of the order of $(5 \div 10)\ \text{cm}^{-1}$, taking into account in the theory only the first term of the expansion is legitimate, if we consider $f(\overline{w}_1)$ pulses with time duration $\Delta\tau \approx (k')^{-1}$ larger than $(10^{-11} \div 10^{-12})$ s, namely pulses generated by the common mode-locked lasers. We determine $C_2(\overline{w})$ for a pulse $f(\overline{w}_1)$ of finite length by imposing the condition $\varrho_q(z, t) = 0$ at $t = -\infty$. The free solution of eq. (15) disappears and the general solution is given by the following expressions:

$$\text{(17}a\text{)}\qquad \begin{cases} \varrho_q(z, t) = \dfrac{g}{4\Gamma'} \{[f(\overline{w}_1)]^2 \operatorname{cosech}^2 [G_1 f(\overline{w}_1)(z - \bar{z}(\overline{w}_1))]\},\\[2ex] \varrho_q(z, t) = \dfrac{g}{4\Gamma'} \{[f(\overline{w}_1)]^2 \operatorname{sech}^2 [G_1 f(\overline{w}_1)(z - \bar{z}(\overline{w}_1))]\}, \end{cases}$$

valid respectively for SFG and DFG, again having kept the useful notation $\overline{w}_1 = t - z/v_1$.

The time evolution of the solutions (17*a*) corresponding to the conditions $f(z, t) \equiv \operatorname{sech}[k(z - v_1 t)]$ and $\bar{z}(\overline{w}_1) \equiv \text{const}/[G_1 f(\overline{w}_1)]$ is shown in fig. 1 and 2. Figure 1 shows that the polariton density spatial distribution in SFG is always decreasing quasi-exponentially in space and time and does not reproduce the shape of the exciting optical pulse. In the case of DFG, if $\bar{z} > 0$, the solution is represented by a pulse having a shape that is rapidly changing in time but that keeps quasi-stationary in space the position of its absolute maximum. For a regular symmetric pulse $f(\overline{w}_1)$ having its maximum at $\overline{w}_1 = 0$ and for $\bar{z}(\overline{w}_1) f(\overline{w}_1) G_1 \equiv \eta(\overline{w}_1) = \text{const}$, the polariton density function reaches its absolute maximum at the co-ordinate $z = \bar{z}(0) = \eta/(G_1 f(0))$ and at the time $t = \bar{z}(0)/v_1$. For $t > \bar{z}(0)/v_1$, the polariton pulse spreads out in space at a rate proportional to the coupling parameter G_1. That same quantity determines the width of the zone of maximum $\varrho_q(z, t)$, if the length of the pulse $f(\overline{w}_1)$ is larger than $1/G_1 f(0)$, and it is proportional to the maximum value of $\varrho_q(z, t)$, which

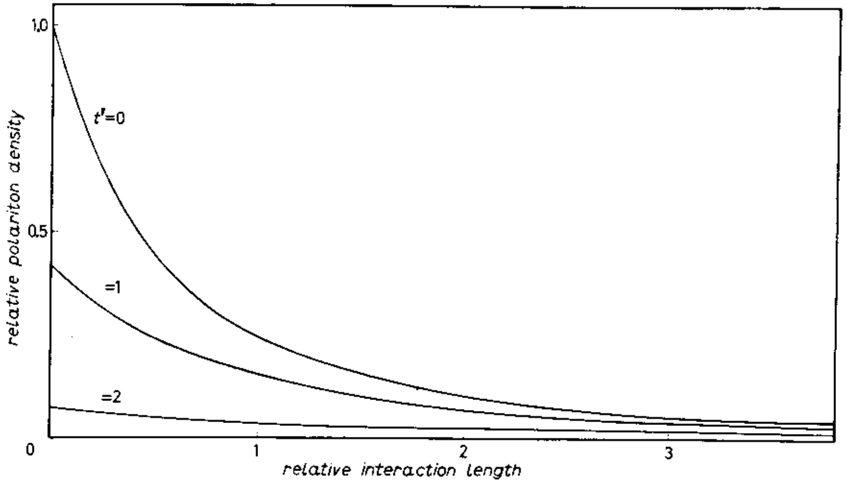

Fig. 1. – Time evolution of the polariton density pulse ϱ_q created by sum frequency generation and corresponding to the driving pulse $\varrho_1(z,t)=\varrho_2(z,t)=\frac{1}{2}\operatorname{sech}k(z-v_1t)$. The above curves are drawn as functions of the dimensionless quantities $z'=kz$, $t'=kv_1t$ and correspond to $G_1/k=1$.

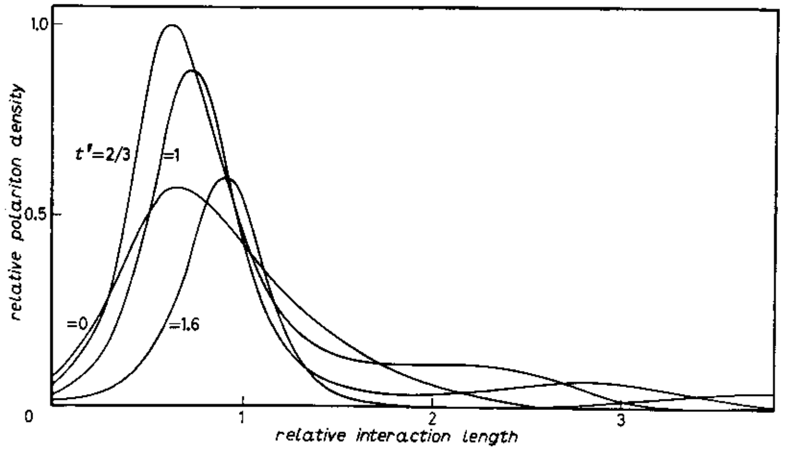

Fig. 2. – Time evolution of the polariton density pulse ϱ_q created by difference frequency generation and corresponding to the driving pulse $f(z,t)=\operatorname{sech}k(z-v_1t)$ and to the condition $\bar{z}(\bar{w}_1)=\eta/(G_1f(\bar{w}_1))$, η being constant. The above curves are drawn as functions of the dimensionless quantities $z'=kz$, $t'=kv_1t$ and correspond to the following values of the parameters: $\eta=2$ and $G_1/k=3$. We note that the maximum value of ϱ_q is reached at the time $t'=\eta k/G_1$ and at the co-ordinate $z'=\bar{z}'(0)=t'$.

is equal to $g/(4\tilde{\Gamma}')$. Obviously more complex situations arise when η is a variable function of $\bar{w}_1$.

Owing to the above considerations, we can conclude that the effect of IR generation on the excitation of polaritons is a somewhat critical process, in particular when short pulses (*e.g.* generated by mode-locked lasers) are made to interact in a highly nonlinear medium. Referring to the conditions corresponding to fig. 2, we notice that the maximum value of $\varrho_q(z,t)$ will never be reached during the interaction if the co-ordinate $\bar{z}(0)$, which depends on the amplitude of the optical fields, lies outside the nonlinear crystal. Furthermore, when the DF pulse emitted from a crystal of length L is detected in the forward direction, the maximum efficiency of the DFG process corresponds to the condition $\bar{z}(0)\simeq L$, namely the exciting fields before the interaction must be related as follows: $\varrho_1^0(\bar{w}_1)\simeq\varrho_2^0(\bar{w}_1)\exp[G_1f(0)L]$. Similarly, when the DF wave is detected in the backward direction owing to a process of nonlinear reflection from the entrance boundary located at $z=0$ (see ref. [1]), the maximum efficiency corresponds to $\bar{z}(0)=0$ and $\varrho_1^0(\bar{w}_1)=\varrho_2^0(\bar{w}_1)$. The propagation theory we have just formulated is greatly simplified if we consider in the equations $\varepsilon(\bar{w}_1)=\text{const}$ and $f(\bar{w}_1)\equiv\varrho^0=\text{const}$, *i.e.* if we are dealing with the steady-state interaction of the fields. In that case eq. (17*a*) may be rewritten in the following form:

$$(17b)\qquad \left|\begin{aligned}&\varrho_q(z)=\frac{(\varrho^0)^2g}{4\xi\tilde{\Gamma}'}\operatorname{cosech}^2\{\varrho_0G_2(z-\bar{z})\} &&\text{(DFG)}\,,\\ &\varrho_q(z)=\frac{(\varrho^0)^2g}{4\xi\tilde{\Gamma}'}\operatorname{sech}^2\{\varrho^0G_2(z-\bar{z})\} &&\text{(SFG)}\,,\end{aligned}\right.$$

where $\xi\equiv n_1/n_2$, $\varrho^0=\varrho_1^0\pm\varrho_2^0\xi$, $\varrho_1^0\equiv[\varrho_1(z)]_{z=0}$, $\varrho_2^0\equiv[\varrho_2(z)]_{z=0}$ are the fields at the crystal boundary. $G_2=g_2/(4v_2)$ and $\bar{z}=(2G_2\varrho^0)^{-1}\ln y$, where $y\equiv\varrho_1^0/(\xi\varrho_2^0)$. Again, $\bar{z}$ is always negative and different from zero for SFG, but can be of either sign for DFG. Furthermore, for SFG, the maximum value of $\varrho_q(z)$ is reached at $z=0$: $\varrho_q(0)=\varrho_1^0\varrho_2^0g/\tilde{\Gamma}'$, further decreasing quasi-exponentially with $z>0$ as shown in fig. 1. For DFG we have again $\varrho_q(0)=\varrho_1^0\varrho_2^0g/\tilde{\Gamma}'$, but the maximum value of $\varrho_q(z)$ is larger if $\bar{z}>0$, and is given by $(\varrho_q)_{\max}\equiv\varrho_q(\bar{z})=\varrho_q(0)(y+1)^2/(4y)$. We verify that, for $y=1$, $\bar{z}=0$ and $(\varrho_q)_{\max}=\varrho_q(0)$.

The general formulation in terms of polariton particles we have adopted has led us to build a transient propagation theory that applies entirely to the pure Raman and 2-photon absorption interaction [13, 14]: $\omega_0=\omega_1\pm\omega_2$, even when the lattice or electronic oscillator is not e.m. active. In that case $\varrho_q(z,t)$ has to be interpreted as the space-time distribution of the density of the crystal excitation in the medium. In the absence of spatial dispersion (*e.g.* Raman scattering from 0-phonon and 2-photon absorption from impurity levels), the phase-matching condition $\Delta\boldsymbol{k}=0$ is always satisfied for e.m. inactive transitions and we can set $\alpha(\omega)=0$ owing to (6). In that case the quantity $\varrho_q(\omega)=(\varrho^0)^2g/4\xi\tilde{\Gamma}'$ appearing in (17*b*) may be conveniently expressed as a function of the frequency mismatch $\Delta\omega = \omega_1 \pm \omega_2 - \omega$ in the following form:

$$\bar{\varrho}_q(\omega) = \frac{\pi\hbar\omega_1\omega_2\omega_0(\varrho^0)^2}{2n_1^2n_2^2}\,\frac{Sd_Q'^2}{(\Delta\omega)^2+\Gamma^2}\,\frac{\Gamma}{\Gamma'}\,. \tag{18}$$

We have introduced in eq. (18) the strength of the oscillator $S \equiv \omega_p^2/\omega_0^2 \equiv \beta\varepsilon_\infty$ and $d_Q' \equiv d_Q/e^*$, where $\omega_p = (4\pi Ne^{*2}/\mu)^{\frac{1}{2}}$ is the plasma frequency. We have shown above that, for the Raman effect, $\varrho_q(0)$ coincides with the maximum value $(\varrho_q)_{\max}$ of the exciton density created in the medium if $\bar{z} \geqslant 0$, while for 2-photon absorption $(\varrho_q)_{\max} = \varrho_q(0)$ and $(\varrho_q)_{\max} = \bar{\varrho}_q(\omega)[4y/(y-1)^2] < \bar{\varrho}_q(\omega)$.

The most complete expression for $\bar{\varrho}_q(\omega)$ valid for e.m. active excitations, in the presence of spatial dispersion, is the following [2]:

$$\bar{\varrho}_q(\omega) = \bar{\varrho}_q(\omega_0)\,\frac{[D'+C\omega_0^2]^2[D'^2+\beta\omega_0^4]}{C^2\beta\omega_0^5\omega^3}\,\frac{[\frac{1}{2}\alpha(\omega)]^2}{|\Delta\boldsymbol{k}|^2+[\frac{1}{2}\alpha(\omega)]^2}\,\frac{[\frac{1}{2}\tilde{\Gamma}(\omega)]^2}{(\Delta\omega)^2+[\frac{1}{2}\tilde{\Gamma}(\omega)]^2}\,, \tag{19a}$$

where

$$\bar{\varrho}_q(\omega_0) = \frac{\pi\hbar\omega_1\omega_2\omega_0(\varrho^0)^2}{2n_1^2n_2^2}\,\frac{Sd_Q'^2}{\Gamma\Gamma'}\,, \tag{19b}$$

after having neglected damping in the expression of D and set $D \simeq D' \equiv \omega_0^2 - \omega^2$. In eq. (19a) spatial dispersion is taken into account by the explicit expression of the group velocity $v_g = \partial\omega/\partial k$ that relates $\tilde{\Gamma}(\omega)$ to $\alpha(\omega)$ according to eq. (6). If we are dealing with an exciton state with small k near the valence band edge of a cubic semiconductor, assuming a diagonal tensor for ε_∞ and lack of degeneracy in $\omega_0(\boldsymbol{k})$, the group velocity is approximately given by [15]

$$v_g = \frac{1}{\partial k/\partial\omega} \approx \frac{c}{\sqrt{\varepsilon_\infty}}\left[1+\frac{\beta}{4}\left(\frac{\omega_0(\boldsymbol{k})}{\omega_0(\boldsymbol{k})-\omega}\right)^2\right]^{-1} \quad \text{for } |\omega_0-\omega| > \beta\omega\,. \tag{20}$$

3. – Electromagnetic fields in the medium. Nonlinear gain.

The formulation in terms of polariton particles adopted in section **2** does not permit a complete description of the generated e.m. field in the medium. The above analysis must be completed by additional conditions that lead to reflected and transmitted electromagnetic waves at the boundaries of the crystal at the fundamental frequencies ω_1, ω_2 as well as at the frequency of the wave ω_3. In this section we shall deal with classical waves rather than photons, in order to take into account the phase of the fields and to consider in a more transparent way the kinematics of the process. We limit ourselves here to considering a steady-state regime for the field, namely the value of the interaction path L in the medium is supposed to be much smaller that the width of the driving pulse $f(\bar{w}_1)$ and of the value of the coupling parameter $[G_1 f(0)]^{-1}$. Furthermore, we make the simplifying hypothesis that the optical fields at frequencies ω_1 and ω_2 are not affected by the nonlinear « gain » or « absorption » processes. The propagation equation of the polariton field at the frequency ω_3 may be written as follows:

$$\left\{\begin{aligned} &\left[\nabla^2+\left(\frac{\omega_3}{c}\right)^2\varepsilon_\infty\right]\boldsymbol{E}_q(\omega_3) = -4\pi Ne^*\left(\frac{\omega_3}{c}\right)^2\boldsymbol{Q}(\omega_3) - 4\pi\left(\frac{\omega_3}{c}\right)^2\boldsymbol{P}^{\mathrm{NL}}(\omega_3)\,,\\ &\mu D(\omega_3)\boldsymbol{Q}(\omega_3) = e^*\boldsymbol{E}_q(\omega_3) + \boldsymbol{F}^{\mathrm{NL}}(\omega_3)\,. \end{aligned}\right. \tag{21}$$

$\boldsymbol{F}^{\mathrm{NL}}(\omega_3)$ and $\boldsymbol{P}^{\mathrm{NL}}(\omega_3)$ are, respectively, the nonlinear force and polarization, that can be defined in terms of the nonlinear energy density U^{NL} in the following way:

$$\left\{\begin{aligned} \boldsymbol{F}^{\mathrm{NL}}(\omega_3) &= -\frac{\partial U^{\mathrm{NL}}}{\partial[N\boldsymbol{Q}^*(\omega_3)]}\,,\\ \boldsymbol{P}^{\mathrm{NL}}(\omega_3) &= -\frac{\partial U^{\mathrm{NL}}}{\partial\boldsymbol{E}_q^*(\omega_3)}\,. \end{aligned}\right. \tag{21b}$$

According to HENRY and GARRETT [5], U^{NL} may be expressed for DFG in the following form:

$$U^{\mathrm{NL}} = -\left[\underline{\boldsymbol{d}}_E : \boldsymbol{E}_1(\omega_1)\boldsymbol{E}_2^*(\omega_2)\boldsymbol{E}_q^*(\omega_3) + N\underline{\boldsymbol{d}}_Q : \boldsymbol{E}_1(\omega_1)\boldsymbol{E}_2^*(\omega_2)\boldsymbol{Q}^*(\omega_3) + \text{c.c.}\right]. \tag{22}$$

Generalization of (22) to SFG is obvious. We verify that eq. (22) is consistent with the definition of the Hamiltonian density given in eq. (4). The tensor nonlinear coupling coefficients appearing in eq. (22) may be taken, to the first approximation, as real and frequency independent over a large range of frequencies centred on ω_0. The complete solution of eq. (21) is a linear superposition of the solutions of the homogeneous Maxwell equation, written in terms of the electric fields, and of the inhomogeneous one. We consider, in the present section, the parametric excitation of a polariton wave in a nonlinear cubic crystal bounded by two plane faces that are not necessarily parallel. We assume that the linear medium in which the crystal is immersed has refractive index $n \simeq 1$ and that the optical fields $\boldsymbol{E}_1(\omega_1)$ and $\boldsymbol{E}_2(\omega_2)$ are undamped infinite plane waves interacting through the entire thickness of the crystal. They give rise, in the crystal, to a nonlinear polarization $\boldsymbol{P}^{\mathrm{NL}}(\omega_3) = \boldsymbol{p}P^{\mathrm{NL}}(\omega_3)$. We limit ourselves to considering the case in which the (real) wave vectors $\boldsymbol{k}_1$ and $\boldsymbol{k}_2$ of the optical fields in the medium belong to the same incidence plane, which is orthogonal to the crystal boundaries, with $\boldsymbol{p}$ orthogonal to that plane.

A particular solution $\boldsymbol{E}_3(\omega_3)$ of eq. (21) may be given in the following form:

$$\boldsymbol{E}_s(\omega_3) = \frac{[d_E' + d_Q'(\omega_p^2/D)]|E_1E_2|}{(k_sc/\omega_3)^2-(\varepsilon_\infty+\omega_p^2/D)}\left(\boldsymbol{p}-\frac{\boldsymbol{k}_s(\boldsymbol{k}_s\cdot\boldsymbol{p})}{k_T^2}\right)\exp[i(\boldsymbol{k}_s\cdot\boldsymbol{r}-\omega_3t)] + \text{c.c.} \tag{23}$$

We have introduced in eq. (23) the notation for the moduli of the vectors: $E_i \equiv |\boldsymbol{E}_i|$, $k_i \equiv |\boldsymbol{k}_i|$, etc. In our particular case the term $k_s(k_s \cdot p)/k_T^2$ is zero throughout the crystal. The wave vector of the driving polarization wave is

$$\boldsymbol{k}_s = \boldsymbol{k}_1 \pm \boldsymbol{k}_2 \equiv (n_s \omega_3/c)(\boldsymbol{k}_s/k_s)\,, \qquad n_s^2 \equiv \varepsilon_s\,, \qquad k_T^2 \equiv \left(\frac{\omega_3}{c}\right)^2 (\varepsilon_\infty + \omega_p^2/D)\,,$$

and the nonlinear coefficients are rewritten in the form $d_E' = 4\pi d_E$, $d_Q' = d_q/e^*$. The solution of the homogeneous Maxwell equation for the ω_3-field near the entrance boundary is composed of a transmitted wave $\boldsymbol{E}_T(\omega_3)$, travelling in the nonlinear medium with wave vector $\boldsymbol{k}_T = \boldsymbol{k}_T' + i\boldsymbol{k}_T''$, and a nonlinearly reflected wave $\boldsymbol{E}_R(\omega_3)$, travelling in the backward direction, in the linear medium. If we call φ_s', φ_T', φ_R' the angles made by the $\boldsymbol{k}_s$, $\boldsymbol{k}_3 \equiv \boldsymbol{k}_T'$, $\boldsymbol{k}_R \equiv n(\omega_3/c)\,\boldsymbol{k}_R/k_R$ wave vectors with the $\boldsymbol{z}$-axis as defined above, the continuity of the transverse components of the momenta of the waves at the boundary leads to the generalized Snell equations $n_s \sin\varphi_s' = n_T \sin\varphi_T' = n \sin\varphi_R'$, where $n_T = n_T'(\omega_3) + i n_T''(\omega_3)$ is the complex refractive index of the nonlinear medium at the frequency of the wave created in the medium. We can show that, in a zone of large dispersion of the linear response of the medium, the $\boldsymbol{k}_T'$ wave is an inhomogeneous wave. In order to show that, it is convenient to express $\cos\varphi_T'$ in the form $\cos\varphi_T' = p \exp[i\psi]$. Expressions for p and ψ in terms of the relative (scalar) phase mismatch $\Delta = (n_s - n_T'(\omega_3))/n_T'(\omega_3)$ and of the relative absorption parameter $\delta = n_T''(\omega_3)/n_T'(\omega_3)$ of the nonlinear medium are immediately obtained from the generalized Snell equation given above:

$$\left\{\begin{aligned} & p^2 \cos 2\psi = 1 - (1+\Delta)^2 \frac{1-\delta^2}{(1+\delta^2)^2} \sin^2\varphi_s'\,, \\ & p^2 \sin 2\psi = \frac{2\delta(1+\Delta)^2}{(1+\delta^2)^2} \sin^2\varphi_s'\,. \end{aligned}\right. \tag{24}$$

Furthermore, the spatial argument of the $\boldsymbol{k}_T$-wave, $\boldsymbol{k}_T \cdot \boldsymbol{r}$, may be written in the following form:

$$\begin{aligned} \boldsymbol{k}_T \cdot \boldsymbol{r} &= k_T(x \sin\varphi_T' + z \cos\varphi_T') = \\ &= k_T'\{x(1+\Delta)\sin\varphi_s' + zp[(\cos\psi - \delta\sin\psi) + i(\sin\psi + \delta\cos\psi)]\}\,, \end{aligned} \tag{25}$$

x and z being the spatial co-ordinates corresponding, respectively, to the $\boldsymbol{x}$-axis, belonging to the incidence plane and to the boundary plane, and to the $\boldsymbol{z}$-axis.

We verify that the surfaces of constant amplitude of the $\boldsymbol{k}_T$-wave are given by $z = \text{const}$ and are therefore planes parallel to the boundary. The surfaces of constant real phase are given by $x(1+\Delta)\sin\varphi_s' + zp(\cos\psi - \delta\sin\psi) = \text{const}$ and are planes whose normals make an angle φ_T'' with the z-axis, where

$$\left\{\begin{aligned} \cos\varphi_T'' &= \frac{p(\cos\psi - \delta\sin\psi)}{[(1+\Delta)^2\sin^2\varphi_s' + p^2(\cos\psi - \delta\sin\psi)^2]^{\frac{1}{2}}} \simeq (1 - \Delta\,\mathrm{tg}^2\varphi_s')\cos\varphi_s'\,, \\ \sin\varphi_T'' &= \frac{(1+\Delta)\sin\varphi_s'}{[(1+\Delta)^2\sin^2\varphi_s' + p^2(\cos\psi - \delta\sin\psi)^2]^{\frac{1}{2}}} \simeq (1+\Delta)\sin\varphi_s'\,. \end{aligned}\right. \tag{26}$$

The simplified expressions appearing in eq. (26) correspond to assuming $\Delta \ll 1$, $\delta \ll 1$ and $\Delta\,\mathrm{tg}^2\varphi_s' \ll 1$. With these approximations, the planes of equal amplitude are still given by $z = \text{const}$ and the direction of the normal to the constant-phase planes is determined by Δ and not by δ. However δ is still responsible for the inhomogeneous character of the wave, owing to eq. (24). The following simplified expression for $\boldsymbol{k}_T \cdot \boldsymbol{r}$ holds:

$$\boldsymbol{k}_T \cdot \boldsymbol{r} \simeq k_T'[x(1+\Delta)\sin\varphi_s' + z\cos\varphi_s'(1 - \Delta\,\mathrm{tg}^2\varphi_s') + iz\delta/\cos\varphi_s']\,. \tag{27}$$

The intensities of the $\boldsymbol{k}_R$ and $\boldsymbol{k}_T$ fields are found by writing the continuity equations for the electric and magnetic fields at the boundaries. Furthermore, the continuity condition for the transverse components of the momenta, expressed by the generalized Snell equation given above, leads to the condition of real propagation of the fields. For the reflected field, that condition is $\sin\varphi_R' \ll 1$, leading to the following one: $\sin\varphi_s' \leqslant [n_T'(\omega)(1+\Delta)]^{-1}$. The amplitude of that wave is found to be

$$E_R = \frac{[d_E' + d_Q'(\omega_p^2/D)](n_s\cos\varphi_s' - n_T\cos\varphi_T')}{(\varepsilon_s - \varepsilon_T)(n\cos\varphi_R' + n_T\cos\varphi_T')}\,|E_1 E_2^*|\,. \tag{28}$$

In the vicinity of the reststrahl band the condition of real propagation for the $\boldsymbol{k}_R$-field leads us to consider only very small angles φ_s', φ_R', φ_T'. For normal reflection and for Δ, δ and n/n_T' much smaller than 1, the amplitude of the reflected field may be written in a simple and significant way:

$$E_R \simeq \frac{d_E'|E_1 E_2^*|}{2\varepsilon_\infty}\,\frac{D + C\omega_0^2}{D + \beta\omega_0^2}\,, \tag{29}$$

where $\beta = \omega_p^2/(\omega_0^2\varepsilon_\infty) = S/\varepsilon_\infty$, and $C = Sd_Q'/d_E'$ is the nonlinear parameter we have defined above. We verify that, with the given approximations, the reflected field is proportional to the ratio of the nonlinear contribution to the dielectric constant at frequency ω_3 and of the same (linear) dielectric constant. A measurement of the intensity and of the phase of the nonlinearly reflected wave as a function of ω_3 would lead to a direct measurement of the parameter $C(\omega_3)$ that characterizes the nonlinear response of the crystal. By introducing the field $E_s = [d_E'(1 + C\omega_0^2/D)/(\varepsilon_s - \varepsilon_T)]|E_1 E_2|$, a nonlinear reflectivity

$R = |E_R|^2/|E_s|^2$ can be defined that is formally identical to the usual expression of the linear reflectivity of linear optics [16], provided we reinterpret, in an obvious way, the quantities n_s and φ_s' appearing in eq. (28). The simple expression (29) obviously does not hold for ω_3 lying in the reststrahl band in which $\Delta \gg 1$. It must be replaced by a more involved and less transparent expression. Of course, as far as nonlinear reflectivity is concerned, the reststrahl band keeps most of its well-known linear properties in the nonlinear regime. We shall consider later in the paper the polariton modes that propagate in the restrahl band (surface polaritons). The wave travelling into the nonlinear medium comes from the interference of the solution $\boldsymbol{E}_s$ given by eq. (23) with the transmitted (inhomogeneous) wave E_T' which is the solution of the homogeneous propagation eq. (21). In the case in which the nonlinear polarization is orthogonal to the incidence plane defined by $\boldsymbol{k}_1$ and $\boldsymbol{k}_2$ and for $\Delta \ll 1$, we are led to the complete solution of eq. (21) through the continuity equations for the electric and magnetic fields at the boundary. If we write the transmitted wave in the form of a plane wave, the complete solution may be given in the following form:

$$\boldsymbol{E}_q(\omega) = \frac{\boldsymbol{p} d_{\boldsymbol{z}}'(1 + C\omega_0^2/D)|E_1 E_2^*|}{2n_T'(\Delta + i\delta)} \exp[i\boldsymbol{k}_s\cdot\boldsymbol{r}]\cdot \\ \cdot\{1 - A_T \exp[-k_T'(\delta + i\Delta)(z/\cos\varphi_s')]\}, \tag{30}$$

where

$$A_T = \frac{n\cos\varphi_R' + n_s\cos\varphi_s'}{n\cos\varphi_R' + n_T\cos\varphi_T'} \simeq \frac{n_s - n - [n_s^2/(2n)]\sin^2\varphi_s'}{n_T + n - [n_s^2/(2n)]\sin^2\varphi_s'}. \tag{31}$$

Equations (30) and (31) correspond to the condition $|\varphi_s'| \ll \pi/2$. We can verify in (30) that the surfaces of constant amplitude of the wave $\boldsymbol{E}_q$ are planes parallel to the boundary. We can also verify that the phase-matching parameter $\Delta \ll 1$, which affects in a quasi-resonant way the undamped transmitted wave, appears in the exponential argument of the free solution and in the expression of A_T. The approximate expression of A_T given in (31), valid for φ_s' small, may be further simplified by setting $\varphi_s' = 0$, $n = 1$, $\delta \ll 1$, $\Delta \simeq 0$. In that case it reduces to the simple equation $A_T \simeq 1 - i\delta$, which corresponds to the simplified expression of $\boldsymbol{E}_R$ given in (28). As we remarked above, it is interesting to take into consideration the particular wave solution $\boldsymbol{E}_s$ of the propagation equation, because, in the approximation that neglects parametric gain effects and for an interaction length L much larger than $(k_T'')^{-1}$, it gives the amplitude of the e.m. part of the polariton wave generated in the crystal. In eq. (30) we can verify that, in the range of polariton frequencies in which phase matching of the interaction can be achieved and for $\delta \ll 1$, the driven-wave intensity $\boldsymbol{E}_s^2$ is a Lorentzian function of Δ if k_T'' is independent of k_T'. This behaviour has recently suggested to us the use of the coherent excitation of the polaritons as a means of studying the optical linear and nonlinear responses of the crystal near the reststrahl band; a zone in which the large optical absorption of the medium does not in practice allow accurate measurements of the optical parameters by the usual methods of the linear spectroscopy of solids. Obviously, the above considerations refer to a behaviour of the parametric mixing processes which is quite general in nonlinear optics. They apply to experiments involving all kinds of e.m. active elementary excitations, such as optical phonons, acoustic phonons, magnons, plasmons, excitons, etc. In the case of perfect phase matching $\Delta = 0$, the amplitude of the driven solution appearing in eq. (30) may also be written in the following simple form:

$$\boldsymbol{E}_s = i\,\frac{d_{\boldsymbol{z}}'|E_1 E_2|}{\varepsilon_\infty \beta \Gamma \omega_3 \omega_0^2}\, D^*(D + C\omega_0^2), \tag{32}$$

where $\beta = S/\varepsilon_\infty$. Thus far we have discussed the propagation of the general solution of the Maxwell equation for the e.m. field created in the medium, disregarding the final process of the emission of that field out of crystal. The study of this process does not present particular complications. As far as the free solution is concerned, the usual Fresnel refraction theory applies without modifications [16]. The same theory is nevertheless not valid in general for the driven solution and it must be substituted by the more involved analysis we have previously adopted in connection with the nonlinear refraction at the entrance boundary. Thus, we are led to consider, in correspondence with the driven solution $\boldsymbol{E}_s$ at the exit boundary, a wave $\boldsymbol{E}_T'$ that is transmitted out of the crystal and a damped inhomogeneous wave reflected back in the medium. In conclusion, the e.m. field, which is created in the crystal slab in a single-pass interaction, comes from the interference of an undamped driven wave with wave vector $\boldsymbol{k}_s$ and two (propagating or evanescent) inhomogeneous waves originating at the boundaries and travelling in the crystal with wave vectors having moduli equal to $n_T'(\omega_3/c)$.

The direction of propagation of the transmitted e.m. field $\boldsymbol{E}_T(\omega)$ is still given by a set of generalized Snell equations analogous to the ones written for the entrance boundary. In addition, analogous considerations on the continuity at the boundary of the electric and magnetic fields lead to the amplitude of the refracted fields. We limit ourselves to giving here, for the sake of completeness, the expression of the field $|\boldsymbol{E}_T'(\omega)|$ that is radiated in a linear medium of refractive index n in a direction making an angle φ with the normal $\boldsymbol{z}'$ to the exit boundary:

$$\boldsymbol{E}_T'(\omega) = \boldsymbol{E}_s(\omega)\,\frac{n_s\cos\varphi_s + n_T\cos\varphi_T}{n\cos\varphi + n_T\cos\varphi_T}. \tag{33}$$

By analogy with our previous discussion, φ_s and φ_T are now the angles (lying in the range $-\pi/2 \to \pi/2$) made by the wave vectors of the corresponding beams with $\boldsymbol{z}'$.

We have assumed so far that the phase matching of the three-wave interaction can be achieved throughout the polariton region. Actually that process is generally a critical one and can be achieved only in special conditions, if the crystal does not show a suitable optical anisotropy to allow the corresponding well-known method of phase matching [1, 17]. If that condition is not present (*e.g.* in cubic crystals), momentum conservation of the interaction may still be provided, even for collinear kinematics, by the so-called « dispersion » phase matching which is based on the combined effects of the optical dispersion affecting the pump frequencies ω_1, ω_2 and the near-resonance frequency ω_3. We refer the reader to [2] for a detailed discussion of that effect in DFG. We only note here that this process ensures phase matching for ω_3 lying in the lower branch of the polariton dispersion curve for DFG and in the upper branch for SFG, if ω_1 and ω_2 lie in a zone of normal optical dispersion. Dispersion phase matching in the upper branch for DFG and in the lower branch for SFG is possible, but implies that one or both pump frequencies lie in a zone of anomalous dispersion in the crystal, *e.g.* near a strong exciton or impurity resonance.

3'1. *Nonlinear gain.* – Thus far we have neglected the effect of the nonlinear gain on the dynamics of the process of polariton generation. Nevertheless we have seen that this effect becomes important when high fields and long interaction lengths are present. An expression for the gain may be derived from eqs. (7*b*) and (9*b*) by applying the classical arguments we have adopted in the present section. We assume here that $\tilde{\Gamma}'(\omega) = \tilde{\Gamma}(\omega)$, $\tilde{\Gamma}(\omega_0) \equiv \Gamma$ and we write $\tilde{\Gamma}(\omega) = \Gamma\beta\omega_0^2\omega^2 \times [D'^2 + \beta\omega_0^4]^{-1}$, owing to (6) and the Huang dispersion relation for $v_v(\omega)$ and $\alpha(\omega)$ [6]. We find that the gain g affecting the polariton wave may be expressed in the following form:

$$g(\omega, \boldsymbol{k}_s) = g_{\max} \frac{\omega_p^4 \omega^6 \Gamma^4}{4c^4 (D')^4} \frac{1}{(\Delta\omega)^2 + [\frac{1}{2}\tilde{\Gamma}(\omega)]^2} \frac{1}{|k_s^2 - (\omega/c)^2(\varepsilon_\infty + \omega_p^2/D)|^2}, \tag{34}$$

where

$$g_{\max} = \frac{h\omega_1\omega_2\omega_p^2}{n_1^2 n_2^2 \omega\Gamma} \left| \frac{D'}{\omega_p^2} d'_E + d'_Q \right|^2 \tag{35}$$

is the expression for the maximum gain, which is reached when $\Delta\omega = \omega_1 \pm \omega_2 - \omega$ and $|\boldsymbol{k}_s| \equiv |\boldsymbol{k}_1 \pm \boldsymbol{k}_2| = |\boldsymbol{k}'_T|$, *viz.* when $\{(\omega_1 \pm \omega_2), k_s\}$ lie on the undamped polariton dispersion curve. A similar conclusion has been reached in ref. [5] for the gain g_2 affecting the $\boldsymbol{k}_2$-wave in stimulated scattering. In that work, an expression for g_2 similar to our $g_{\max}$ is given. We note that, for $\omega \to \omega_0$, the effect of the electronic nonlinearity d'_E disappears and we are left with an expression corresponding to the resonant 2-photon absorption coefficient for SFG and to the Raman gain for DFG. Our present theory is valid only if spatial dispersion affecting the excitation associated with the excited polariton wave is considered to be a small effect [18]. If it is not, substantial complications arise in the theory of wave propagation due to the occurrence of « anomalous » waves [19]. We shall develop the theory of gain in the presence of spatial dispersion in an *ad hoc* paper.

4. – 4-photon resonant coherent scattering.

The presence of the coherent polariton wave created by SFG or DFG in the medium may be probed either by direct detection of the generated e.m. field at frequency $\omega_3 = \omega_1 \pm \omega_2$ and transmitted out of the medium, or by means of a resonant 4-photon coherent inelastic-scattering process. In spite of the higher-order nonlinear process involved, this new kind of experiment generally proves to be easier, for the purpose of the polariton wave detection, than the corresponding direct SF or DF 3-wave mixing experiment, because surface effects are generally negligible and, more important, because we can by this process up or down convert the polariton wave in a zone of the optical spectrum where absorption of the crystal is negligible and where fast and sensitive detectors are operating. Furthermore, we should stress the intrinsic physical interest of this effect, which allows the study of some linear and nonlinear properties of the crystal not generally accessible by other methods of spectroscopy. This process also suggests entirely new methods of nonlinear spectroscopy such as the ones devised for the study of the near-resonance dispersion of the nonlinear optical susceptibilities of crystals [2, 9, 20] and the solid-state spectroscopy *in momentum space* that has been applied for the first time in optics by the Quantum Optics Group in Orsay [20]. The diagrams of the possible kinematical configurations for this process are shown in fig. 3 for SF and DF excitations.

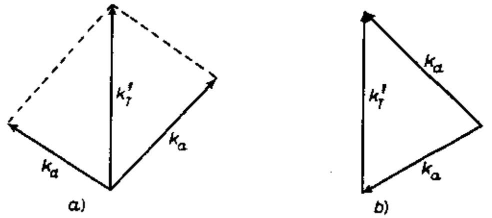

Fig. 3. – Kinematics of the polariton wave $\boldsymbol{k}'_T$ coherent-scattering schemes. The $\boldsymbol{k}'_T$-wave may be excited in turn by either the sum or difference frequency interaction for either scheme. The four possible overall configurations are considered in sect. **5.** *a)* $\boldsymbol{k}'_T = \boldsymbol{k}_d + \boldsymbol{k}_a$, *b)* $\boldsymbol{k}'_T = \boldsymbol{k}_d - \boldsymbol{k}_a$.

The analysis of the present effect is not particularly involved if we make use of the simplifying approximations we have already introduced in the paper, *viz.* transverse plane-wave approximation, monochromaticity for the fields and the scalar representation of the tensor components. Obviously, this last simplifying condition broadens the scope of the present discussion, as it covers the general behaviour of a nonlinear medium, but care is advised in the application of the theory to the case of a particular crystal, even of cubic symmetry.

If we assume that the probing field $\boldsymbol{E}_d(\omega_d, \boldsymbol{r}) = \boldsymbol{E}_d \exp[-i\boldsymbol{k}_d\cdot\boldsymbol{r}]$ is not depleted or amplified along the interaction path, the simple expression for the free-energy density U^{NL} must be rexritten in the following form:

$$U^{\text{NL}} = -\{\underline{d}_E:(\boldsymbol{E}_1\boldsymbol{E}_2^*\boldsymbol{E}_q^* + \boldsymbol{E}_d\boldsymbol{E}_a^*\boldsymbol{E}_q^*) + N\underline{d}_Q:(\boldsymbol{E}_1\boldsymbol{E}_2^*\boldsymbol{Q}^* + \boldsymbol{E}_d\boldsymbol{E}_a^*\boldsymbol{Q}^*)\}\,, \tag{36}$$

while the polariton e.m. field may be written after (23) in the form

$$\boldsymbol{E}_q(\omega_3) = \frac{d'_E + d'_Q\omega_p^2/D}{\Delta\varepsilon}\,(|E_1E_2^*| + |E_dE_a^*|)$$

with $\boldsymbol{E}_d(\omega_a\cdot\boldsymbol{r}) = \boldsymbol{E}_a \exp[-i\boldsymbol{k}_a\cdot\boldsymbol{r}]$ the (weak) optical scattered field generated in the medium and $\Delta\varepsilon \equiv n_s^2 - (\varepsilon_\infty + \omega_p^2/D)$. Equation (36) is written for down-conversion scattering of the field $\boldsymbol{E}_d$ and for DFG. Generalization to other kinematical scattering schemes and for SFG is immediate and does not affect the final results of the theory. We can now apply (21*b*) in order to evaluate the nonlinear polarization $P^{\text{NL}}(\omega_a, \boldsymbol{r}) = P_a^{\text{NL}} \exp[-i\boldsymbol{k}_a\cdot\boldsymbol{r}]$. We finally find the simple expression

$$P_a^{\text{NL}} = \frac{d_E'^2}{4\pi}\left\{\frac{(1 + C\omega_0^2/D^*)^2}{(\Delta\varepsilon)^*} + \frac{C^2\omega_0^2}{SD^*}\right\}E_a|E_d|^2 - \\ - \frac{d_E'^2}{4\pi}\left\{\frac{(1 + C\omega_0^2/D^*)^2}{(\Delta\varepsilon)^*} + \left(\delta + \frac{C^2\omega_0^2}{SD^*}\right)\right\}E_1^*E_2E_d\,. \tag{37}$$

In eq. (37) $\delta = \chi_{\text{NR}}^{(3)}/(N\pi[d_E']^2)$ brings into the theory the contribution of the third-order susceptibility that accounts for the overall coupling of the 4 photons $\boldsymbol{k}_1, \boldsymbol{k}_2, \boldsymbol{k}_d, \boldsymbol{k}_a$. It is not affected by the polariton resonance and can be assumed to be a real quantity, as for d_E', if the interacting optical frequencies are far from other resonances of the medium. The experimental value of δ has been found to be ~ 6 for GaAs [2[illegible]] and ~ 180 for LiNbO$_3$ [22]. The large difference among the two values is not unexpected as δ can be shown, by quantum-mechanical arguments, to be approximately proportional to the inverse of the absorption coefficient of the crystal in the transparency region [23]. Inspection of (37) and of the Maxwell equation for $\boldsymbol{E}_a(\omega_a, \boldsymbol{r})$ leads us to consider a nonlinear correction to the refractive index $\bar{n}_a' = \sqrt{\bar{\varepsilon}_a}$ of the crystal at the frequency ω_a and a nonlinear gain for the scattered field. We find

$$n_a' = \sqrt{\bar{\varepsilon}_a + d_E'^2\frac{C^2\omega_0^2}{\bar{D}'}|E_d|^2}\,,$$

$$\text{gain} = \frac{\omega_a}{c}\,\frac{d_E'^2(\gamma')^2}{2S\omega_0^3\omega_3\,\bar{n}_a'}\,,$$

where $\bar{D}' \equiv \omega_0^2(1 + C) - \omega^2$ and $\gamma_0 = \Gamma/\omega_0$. For $\omega_3 \to \omega_0$ the nonlinear correction to $\bar{n}_a'$ and the gain correspond to the well-known behaviour of the anti-Stokes generation in coherent Raman scattering [1, 24, 25]. The intensity of the $\boldsymbol{k}_a$-beam detected outside the medium may be expressed in the following form:

$$I_a = \frac{4(2\pi\omega_3)^4\omega_a^2}{c^6 n_a'^2}\,I_1I_2I_d|\tilde{d}|^2\left[\sin^2\frac{|\Delta\boldsymbol{k}_a|l}{2}\Big/\left(\frac{|\Delta\boldsymbol{k}_a|l}{2}\right)^2\right]l^2 \tag{38}$$

with

$$|\tilde{d}|^2 = \left|d_E'\left\{\frac{(1 + C\omega_0^2/D^*)^2}{[k_s^2 - (\omega/c)^2(\varepsilon_\infty + \omega_p^2/D^*)]} + \left[\frac{C^2\omega_0^2}{SD^*} + \delta\right]\right\}\right|^2 \tag{39}$$

being the nonlinear coefficient that accounts for the coupling. We can verify that, for $k_s \approx k_T'$, $|k_s^2 - (\omega/c)^2(\varepsilon_\infty + \omega_p^2/D^*)|^{-2}$ approaches a Lorentzian function of $k_s - k_T'$ having its maximum for $k_s = k_T'$. The dependence of I_a on the phase matching of the 3-wave polariton generation process is at the basis of the mentioned spectroscopy in momentum-space [20, 26]. We should nevertheless notice that the second term appearing at the r.h.s. of (39) is generally not negligible compared with the phase-matching resonant one in the same expression. In particular, the two terms are of the same size and $\pi/2$ out of phase for $\omega = \omega_0$ if $\delta = 0$. The effect of this additional term could explain the asymmetry of some of the momentum-space spectral lines we have found in the experiments [20]. The moduli and phases of the two contributions to $|\tilde{d}|^2$ may be easily evaluated on the basis of the nonlinear coefficients of the crystal for each polariton frequency excited and the experimental spectra may therefore be easily reduced to give the correct spectra leading to the study of the polariton dispersion and damping. We note that I_a is proportional to the product of the intensities of the interacting beams and to the function $[\sin\frac{1}{2}|\Delta\boldsymbol{k}_a|l/(\frac{1}{2}|\Delta\boldsymbol{k}_a|l)]^2$ that accounts for the overall phase mismatch $\Delta\boldsymbol{k}_a$ of the four optical waves $\boldsymbol{k}_1$, $\boldsymbol{k}_2$, $\boldsymbol{k}_d$, $\boldsymbol{k}_a$. The value of the function depending on $\Delta\boldsymbol{k}_a$ is always near unity under our experimental conditions [20].

5. – Nonlinear spectroscopy of bulk polaritons.

The present work is not a review paper and therefore we shall not give an exhaustive account of the experimental situation of the branch of nonlinear spectroscopy we are dealing with here. However, before focusing briefly on the author's own work, it seems worth-while to mention some key works performed on the subject.

5'1. *Sum frequency generation* (*resonant second-harmonic generation*). – The first experiment of near-resonance SFG was reported by MAHR and co-workers at Cornell University [27]. In that experiment, a tunable dye laser was used to excite resonantly by SFG the first exciton line in CuCl at 3.215 eV. The result of that experiment shows a resonant behaviour in the nonlinear susceptibility of the crystal in correspondence with the exciton resonance. This work parallels the investigation of the same polariton resonance by 2-photon absorption [28, 29]. An extensive presentation of earlier works on 2-photon absorption spectroscopy may be found in [30].

The 4-photon mixing associated with a SF excitation of the above polariton resonance in CuCl has been reported by Kramer, Parsons and Bloembergen, which investigated experimentally the effect of interference of the third-order light mixing and second-harmonic exciton-polariton generation [31]. We have presented the theory of this effect in sect. **4**. For further details on this work see the lecture of Bloembergen in this volume.

5'2. *Difference frequency generation.* – The first DF mixing experiment of relevance in nonlinear spectroscopy has been reported by Faust and Henry [9]. In that work the dispersion of the nonlinear optical susceptibility near the 0-phonon resonances in GaP has been thorougly studied. Further works on this process have been reported: they correspond to mixing experiments [2, 32] and to stimulated scattering experiments from 0-phonon polaritons [33].

In the author's work [2], two coherent beams generated by tunable lasers were injected in a GaP crystal and the coherent IR radiation corresponding to the 0-phonon polariton excitation was detected outside the crystal. Various measurements were performed in the experiment. The angular distribution of the emitted intensity I_{IR} and the study of the evolution of the e.m. field in the crystal (fig. 4, 5) allowed a set of measurements of the absorption coefficient of GaP in a zone of large absorption ($\lambda_{IR} \approx 35\ \mu m$). Furthermore, the frequency dependence of I_{IR} has led us to the study of the dispersion of the nonlinear susceptibility of GaP in the lower branch of the polariton dispersion curve.

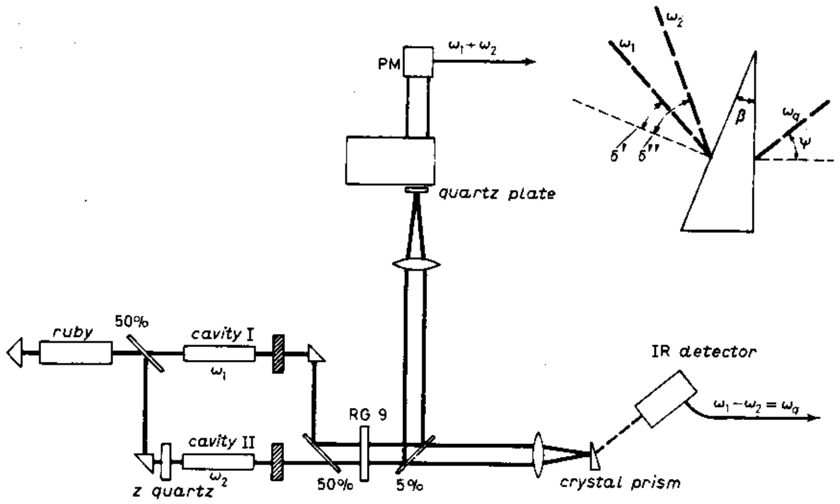

Fig. 4. – Schematic diagram of the bulk polariton DFG apparatus [2].

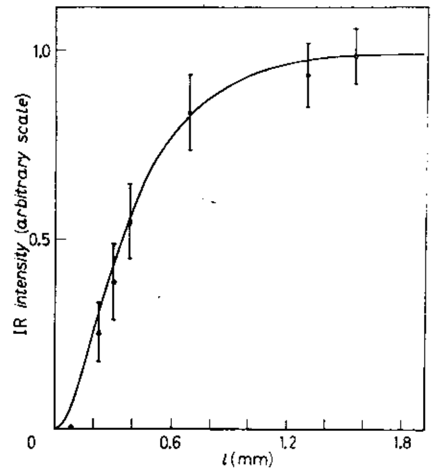

Fig. 5. – Infra-red intensity emitted at $\lambda = 34.6\ \mu m$ in the phase-matching condition as a function of the interaction length l in GaP. The curve directly shows the spatial distribution of the e.m. field in the crystal. $\alpha = 72\ cm^{-1}$, 300 K.

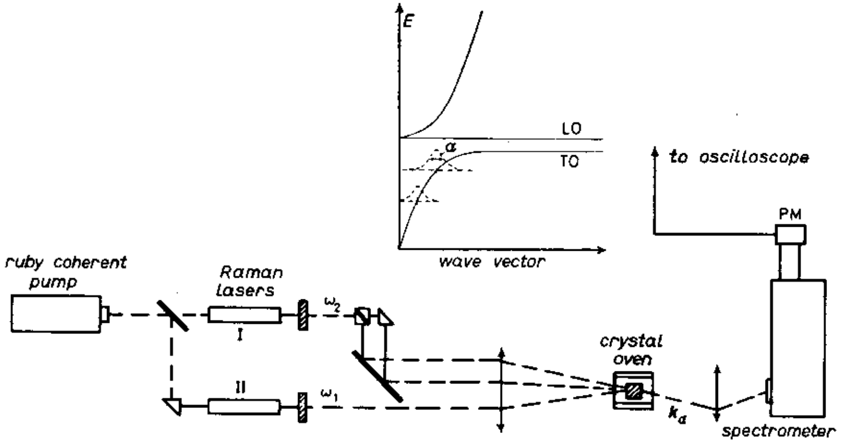

Fig. 6. – Schematic diagram of the **k**-space spectroscopy apparatus [20, 34].

Momentum-space spectroscopy has been performed in GaP at various temperatures (fig. 6) (ref. [20, 26, 34]). At 300 K the lower-branch polariton dispersion curve has been experimentally plotted with the high accuracy that is intrinsic in the method [26]. Furthermore, the absorption coefficient of the crystal has been measured in the near-reststrahl high-reflectivity region, which is hardly accessible to linear methods as far as measurement of this quantity is concerned (fig. 7). The temperature dependence of $|k'_T|$ and α near the TO resonance has been considered for Gap in ref. [34]. It has been found that near $T = 450$ K these two quantities, as well as ω_{TO} and Γ, show a rapid change. That temperature coincides with the Debye temperature of GaP calculated on the basis of the elastic constants [35].

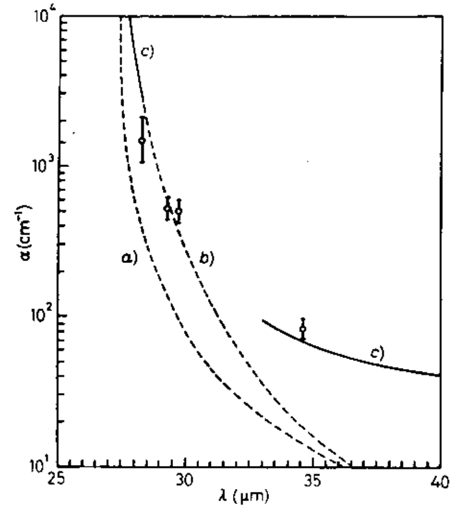

Fig. 7. – Absorption coefficient of GaP (300 K) *vs.* wavelength. Curve *a*) has been drawn on the basis of the IR data reported in ref. [36]. Curve *b*) has been drawn on the basis of the multiple-oscillator model for the damping of the 0-phonon in GaP [37]. Curve *c*) shows the results of a previous experimental investigation on $\alpha(\lambda)$ using conventional linear methods. Upper branch: Kramers-Krönig analysis of reflection experiments. Lower branch: transmission data [38]. Curve *c*) is reported without structure.

The 4-photon coherent-scattering process has been applied to the study of the dispersion of the nonlinear susceptibility in $LiNbO_3$ [22].

The reader can find further discussions on the SFG, DFG, 4-photon scattering experiments and a comprehensive bibliography in the works of BLOEMBERGEN, SHEN and LOUDON published in this volume.

6. – Nonlinear excitation of surface polaritons.

There are situations in which the dielectric constant of the medium, at the frequency ω at which the nonlinear polarization is excited, is negative [36]. The most common situation of this sort is presented by a metal for $\omega < \omega_p$ (plasma frequency) and by a semiconductor crystal for ω lying in the (phonon or exciton) reststrahl band [2, 18]. When this is the case, the driven e.m. fields (*i.e.* the particular solution of the inhomogeneous Maxwell equation which is associated with the driving NL polarization wave) can still propagate in the bulk of the crystal, with a wave vector $\boldsymbol{k}_s = \boldsymbol{k}_1 \pm \boldsymbol{k}_2$ and without attenuation, if the attenuation of the fundamental fields is absent. However, the free solution, which arises at the boundaries, cannot propagate in the bulk because $k''_T(\omega) > k'_T(\omega)$. The only propagating mode in the medium corresponds to an evanescent field which is bound to the surface, propagates with a wave vector $\boldsymbol{k}_x$ parallel to the surface itself and decreases exponentially in the direction z normal to the surface being proportional to [16]

$$\exp[-\bar{\alpha}z]\,, \qquad \bar{\alpha} \equiv \sqrt{k_x^2 - k_0^2\bar{\varepsilon}\bar{\mu}}\,, \qquad k_0 \equiv \omega/c\,.$$

We can verify that for $\bar{\varepsilon} < 0$ (and $\bar{\mu} > 0$) $\bar{\alpha}$ is real for every k_x. Suppose now that the boundary we are considering is an interface between two media: a nonlinear one characterized by $\bar{\varepsilon} < 0$ and a linear one with $\varepsilon > 0$. The free wave can propagate in the bulk of the linear medium if $k_x^2 < k_0^2\varepsilon$. If this equation is not satisfied, a second evanescent wave with $\alpha = \sqrt{k_x^2 - k_0^2}$ travels at the surface in the linear medium with the same wave vector k_x of the wave in medium $\bar{\varepsilon}$. Let us study this situation on the basis of the Maxwell equations written in the neighbourhood of the boundary. Let us consider the excitation of free TM waves on either side of the interface. That one is defined by the (x, y) reference plane, where x is assumed to be the direction of wave propagation. The z-axis is assumed directed toward the $\bar{\varepsilon}$-medium. Assuming harmonic ω-dependence of the fields and $D^{NL} \equiv 4\pi P^{NL} = 4\pi\tilde{P}^{NL}\exp[i\boldsymbol{k}^s\cdot\boldsymbol{r}]$, the relevant Maxwell equations are written in the following form:

$$\left\{\begin{aligned} &\frac{\partial H_y}{\partial z} - ik_0\bar{\varepsilon}E_x = ik_0D_x^{NL}\,,\\ &\frac{\partial H_y}{\partial x} + ik_0\bar{\varepsilon}E_z = -ik_0D_z^{NL}\,,\\ &\frac{\partial E_x}{\partial z} - \frac{\partial E_z}{\partial x} - i\bar{\mu}k_0H_y = 0\,, \end{aligned}\right. \tag{40}$$

for the nonlinear medium $\bar{\varepsilon}$. The equations for medium ε are identical to (40) with $D^{NL} = 0$, $\bar{\mu} \to 1$ and interchange $\bar{\varepsilon} \leftrightarrows \varepsilon$. The solution of the boundary condition problem (continuity across the boundary of E_x and H_y) leads to the following expressions for the fields in the nonlinear medium:

$$(41)\quad \begin{cases} \bar{E}_x(z,x) = \dfrac{-1}{\bar{\varepsilon}[(k_z^s)^2+\bar{\alpha}^2]}\cdot \\ \qquad \cdot\left\{[k_x^s k_z^s D_z^{\mathrm{NL}} + \bar{\alpha}^2 D_x^{\mathrm{NL}}] - \dfrac{\bar{\alpha}}{\bar{\alpha}+\eta\alpha} A \exp[-\bar{\alpha}z]\exp[ik_x^s x]\right\}, \\ \bar{E}_z(z,x) = \dfrac{-1}{\bar{\varepsilon}[(k_z^s)^2+\bar{\alpha}^2]}\cdot \\ \quad \cdot\left\{[(k_z^s)^2-(k_x^s)^2+\bar{\alpha}^2]D_z^{\mathrm{NL}} + [k_x^s k_z^s]D_x^{\mathrm{NL}} - \dfrac{ik_x^s}{\bar{\alpha}+\eta\alpha} A \exp[-\bar{\alpha}z]\exp[ik_x^s x]\right\}, \\ \bar{H}_y(z,x) = \dfrac{k_0}{(k_z^s)^2+\bar{\alpha}^2}\cdot \\ \qquad \cdot\left\{[(k_z^s)D_x^{\mathrm{NL}} - (k_x^s)D_z^{\mathrm{NL}}] - \dfrac{i}{\bar{\alpha}+\eta\alpha} A \exp[-\bar{\alpha}z]\exp[ik_x^s x]\right\}, \end{cases}$$

where

$$\eta \equiv \bar{\varepsilon}/\varepsilon$$

and

$$A \equiv [k_x^s(k_z^s + i\alpha\eta)D_z^{\mathrm{NL}} + (\bar{\alpha}^2 - i\alpha\eta k_z^s)D_x^{\mathrm{NL}}]\exp[-i\boldsymbol{k}^s\cdot\boldsymbol{r}].$$

Expressions (41) show that in the medium $\bar{\varepsilon}$ the fields are the sum of a driven solution and of a « free » solution ($\propto A$). In the linear medium ε only the « free » solution exists:

$$(42)\quad \begin{cases} E_x(x,z) = \dfrac{-\alpha B}{\varepsilon[(k_z^s)^2+\bar{\alpha}^2][\bar{\alpha}+\eta\alpha]}\exp[\alpha z]\exp[ik_x^s x], \\ E_z(x,z) = \dfrac{ik_x^s B}{\varepsilon[(k_z^s)^2+\bar{\alpha}^2][\bar{\alpha}+\eta\alpha]}\exp[\alpha z]\exp[ik_x^s x], \\ H_y(x,z) = \dfrac{-ik_0 B}{[(k_z^s)^2+\bar{\alpha}^2][\bar{\alpha}+\eta\alpha]}\exp[\alpha z]\exp[ik_x^s x] \end{cases}$$

with B obtained from A witht he change (not interchange) $\alpha\eta\to\bar{\alpha}$. We verify that the « free » solutions on either side of the interface diverge for $\bar{\alpha}+\eta\alpha=0$. It is easy to recognize that this equation reduces to the following expression:

$$(43)\qquad k_x^2 = k_0^2\frac{\bar{\varepsilon}\varepsilon}{\varepsilon+\bar{\varepsilon}},$$

which is the dispersion relation for surface polaritons (SP) at the boundary [39-43]. In actual cases $\bar{\varepsilon}$ and/or ε are complex and the expression $[\bar{\alpha}+\eta\alpha]^{-1}$ can be given in a Lorentzian form having a finite width and a finite maximum at $(k_x^s)^2 = k_0^2\,\mathrm{Re}\,(\bar{\varepsilon}\varepsilon/(\bar{\varepsilon}+\varepsilon))$, reproducing the behaviour of the process of bulk polariton nonlinear excitation, eq. (23). In this connection an important point must be clarified. The « free » waves we have just considered and that coexist at the interface with the driven solution *do not* form a surface polariton because they are not « free » of choosing their own wave vector, which is determined by the optical properties of the medium, eq. (43). Their wave vector is in fact determined by the driving NL polarization wave being equal to k_x^s. This situation is entirely different from the one presented by the process of NL excitation of bulk polaritons considered in sects. **2** and **3** of this paper: in that case the k_T-waves are real free waves, *i.e.* polaritons. In order to consider NL generation of real surface polaritons we can think of the realistic situation of a NL polarization wave with finite cross-section at the boundary. Assuming sharp transverse boundaries at the interface, we can consider a new set of e.m. boundary conditions at the surface of the generalized ideal cone which intersects the physical interface between the two media and that represents the separation surface between the regions in which $P^{\mathrm{NL}}=0$ and $P^{\mathrm{NL}}\neq 0$. This boundary condition problem is quite complex, because it must be solved for a tridimensional boundary. However, with the transformations {space→time, k-vectors→frequency}, the situation is similar to the case of the excitation of a harmonic oscillator by an oscillatory force represented by a square pulse in time. Suppose that $\omega_0=\omega_0'+i\omega_0''$ is the complex eigenfrequency of the oscillator and $\omega\sim\omega_0'$ is the real exciting carrier frequency. Just after the time boundary defined by the sharp trailing edge of the force pulse, the frequency of the oscillator jumps from ω to ω_0 and the oscillation intensity, which is resonantly dependent on the frequency matching $\omega^2-\omega_0'^2$, starts decreasing exponentially with a time constant $\tau\sim 1/\omega_0''$. Physically the picture is quite adequate to represent qualitatively the behaviour of the surface polariton at the boundary. The SP intensity is determined at the boundary by the phase matching $(k_x^s)^2 = k_0^2\,\mathrm{Re}\,(\bar{\varepsilon}\varepsilon/(\bar{\varepsilon}+\varepsilon))$, and the SP travelling away from the boundary is damped with an attenuation constant k_x'', which is determined by the following set of equations:

$$(44)\quad \begin{cases} \boldsymbol{k}_x \equiv k_x' + ik_x'' \quad \text{(SP wave vector)} \\ \bar{\varepsilon} \equiv \bar{\varepsilon}' + i\bar{\varepsilon}'', \\ (k_x')^2 - (k_x'')^2 = k_0^2\,\mathrm{Re}\,\dfrac{\varepsilon\bar{\varepsilon}}{\varepsilon+\bar{\varepsilon}}, \\ 2k_x'k_x'' = k_0^2\,\mathrm{Im}\,\dfrac{\varepsilon\bar{\varepsilon}}{\bar{\varepsilon}+\varepsilon}. \end{cases}$$

We can see that k_x'' is determined by the damping of the crystal excitation, *i.e.* by $\bar{\varepsilon}''$. In actual cases k_x'', evaluated by eq. (44), represents the lower limit of the damping constant of the SP wave. That one is also affected by some physical properties of the surface, like the surface roughness, etc. The damping length $l = 1/k''_x$ is of the order of several cm for SP on a metal surface, in the far infra-red, and of a fraction of a mm for SP associated with reststrahlung phonon or exciton bands of a semiconductor.

So far we have considered the process of NL generation of coherent surface polaritons. The driving wave is the NL polarization which can be created, for two-wave interaction, by SFG or DFG. The detection of the coherent polariton can be obtained by a straightforward application of the NL four-photon mixing scheme considered in sect. **4** or by direct coupling of the radiation associated with the polariton at the surface. In this connection let us consider the crystal-vacuum interface, $\varepsilon = 1$. We recall that, owing to eq. (43), $k'_x > k_0$. The SP radiation in the vacuum is associated with an evanescent wave and, for a perfectly plane interface, it can be coupled to a detector away from the surface only by a reverse frustrated total internal reflection (FTR) using a transparent prism placed on the surface at a distance ξ. The FTR method, which has been first applied by Otto [44, 45], is the only linear method for exciting and detecting surface polaritons on a plane surface. It transforms a bulk wave into an evanescent wave with $k_x > k_0$, as required for the excitation of SP, and the evanescent wave associated with a SP into a bulk wave to be detected. We may note that the method is inefficient, because the field energy transferred to (or from) the surface from (or to) the prism is proportional to

$$\exp\left[-2\sqrt{k_x^2 - k_0^2}\,\xi\right] \sim \exp\left[-\frac{4\pi}{\lambda_0}\xi\right]$$

for $k_x \gg k_0$. For $\xi \sim \lambda_0$ the energy transfer is of the order of 10^{-5}. We could prove that the same or a higher efficiency can be obtained with our NL method in which, in the parametric approximation [1], almost the entire energy transferred by the fundamental beams to the NL polarization is in turn transferred to the surface polariton. The theory of the nonlinear excitation of surface polaritons has been worked out by De Martini and Shen [46].

7. – Nonlinear spectroscopy of surface polaritons.

The first experiment on coherent excitation and detection of surface phonon-polaritons (SP) has been reported recently by De Martini, Mataloni, Palange and Shen [47]. In that work the dispersion of the SP wave vector $K_x(\omega) = K'_x(\omega) + iK''_x(\omega)$ in the III-V semiconductor GaP has been investigated by the methods of 4-wave mixing and K-space spectroscopy [20, 26].

The experimental set-up, similar to the one in ref. [20], is shown in fig. 8. A Q-switched ruby laser with a 30 ns pulse width provided a beam at $\omega_1 = 14\,403$ cm^{-1}. It was used to pump simultaneously two dye lasers emitting two tunable beams at ω_2 and ω_3 with a line width of 1.5 cm^{-1}. In the experiment, ω_3 (the probe frequency) was held fixed at 13 333 cm^{-1}, while ω_2 was tuned in the range between 14 006 and 14 035 cm^{-1}, so that optical mixing of ω_1 and ω_2 beams could excite surface polaritons in the reststrahl band of the crystal in the range between 368 and 397 cm^{-1}. Part of the ruby laser beam and the two dye laser beams were focused by a common achromatic lens with 20 cm focal length on the surface of a 2 mm GaP slab. Small diaphrams were used in front of the lens to reduce the convergence angle of each beam at the crystal to $4\cdot 10^{-3}$ rad. The focal spot was about 0.5 mm. The output at $\omega_4 = \omega_3 - \omega_1 + \omega_2$ around the phase-matched direction $\boldsymbol{k}_4 = \boldsymbol{k}_3 - \boldsymbol{k}_1 + \boldsymbol{k}_2$ was collected by a large-aperture lens and analysed by a double-stage Hilger D330/1 monochromator and detected by a RCA C31025C Quantacon photomultiplier. With 50 kW incident beams we detected a resonant output peak power at ω_4 of 0.1 μW. For each given excited SP frequency $\omega_1 - \omega_2$ we measured $I(\omega_4)$ as a function of k^s_x, which is the projection of $\boldsymbol{k}^s = \boldsymbol{k}_1 - \boldsymbol{k}_2$ on the surface of the slab. We found that the experimental curves $I(k^s_x)$ at different ω_4 fitted well a set of Lorentzian curves, as expected from the theory [46]. In fact when $k^s_x \approx K'(\omega)$, the surface wave in the crystal may be expressed in the form [46]

$$E(\omega) = A\,\frac{1}{\Delta k_x - iK''_x}\,(\hat{x}k_{bz} - \hat{z}k^s_x)\,P^{\rm NL}_x(\omega)\exp\left[i(k^s_x x - \omega t) + ik_{bz}z\right], \tag{45}$$

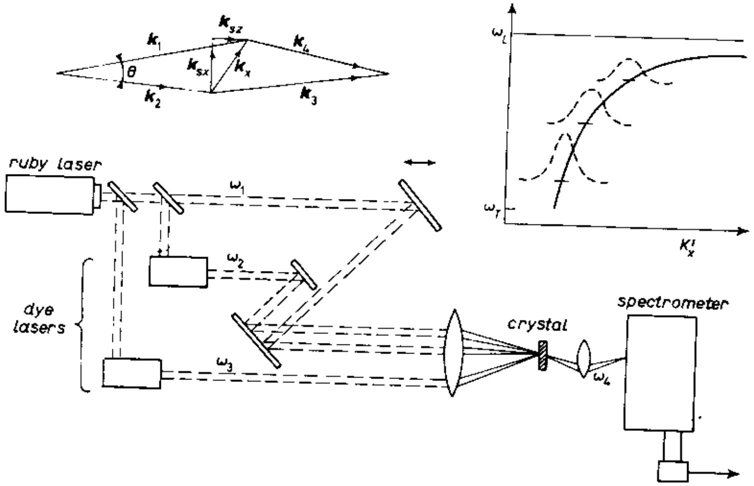

Fig. 8. – Experimental set-up for surface polariton nonlinear excitation.

where

$$
\begin{aligned}
A &= -[2\pi(k_{bz}+\bar{\varepsilon}k_{az})/K'\,\bar{\varepsilon}(1-\bar{\varepsilon}^2)(k^{s^2}-k_b^2)(\bar{\varepsilon}k_{az}k_z^s-k_{bz}^2)]\,,\\
k_b^2 &\equiv \bar{\varepsilon}(\omega/c)^2, \qquad \Delta k_x \equiv k_x^s-K'_x\,,\\
k_{az}^2 &\equiv k_0^2-k_x^{s^2},\\
k_{bz}^2 &\equiv k_b^2-k_x^{s^2},\\
k_0 &\equiv \omega/c\,.
\end{aligned}
$$

$\boldsymbol{P}_x^{\mathrm{NL}}(\omega)=[\chi^{(2)}(\omega):\boldsymbol{E}_1(\omega_1)\,\boldsymbol{E}_2(\omega_2)]_x$ is the x-component of the nonlinear polarization at the difference frequency $\omega=\omega_1-\omega_2$. One can use a third laser beam $E(\boldsymbol{k}_3,\omega_3)$ to probe the excited surface wave [46]. Optical mixing of this probing field with the surface wave induced a nonlinear polarization $P^{\mathrm{NL}}(\omega_4=\omega_3-\omega)$, which in turn generates a new wave $E(\omega_4)$ with an intensity given by

$$
I(\omega_4,\Delta k_x)\propto|\boldsymbol{P}^{\mathrm{NL}}(\omega_4)|^2=\frac{|A|^2}{\Delta k_x^2+K_x''^2}\,|\chi^2(\omega_4):\boldsymbol{E}(\omega_3)\,\chi^{(2)*}(\omega):\boldsymbol{E}^*(\omega_1)\,\boldsymbol{E}(\omega_2)|^2; \tag{46}
$$

$I(\omega_4)$ is a Lonretzian function of k_x having its maximum for $k_x^s=K'_x$ and half-width $2K''_x$. Our experiment gives therefore full information on the linear properties of the surface polariton. In fig. 9 and 10 the experimental data in dispersion of K'_x and K''_x are shown. The solid theoretical curves are obtained

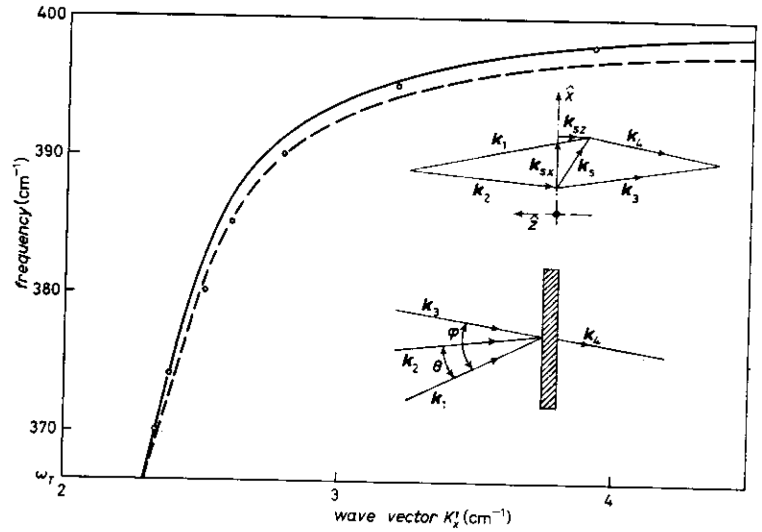

Fig. 9. – Frequency dependence of the surface polariton wave vector $K'(\omega)$.

from a single-oscillator model with the following values of the parameters: $\omega_{\mathrm{TO}}=367.3\ \mathrm{cm^{-1}}$, $\omega_{\mathrm{LO}}=403\ \mathrm{cm^{-1}}$, $\varepsilon_\infty=9.091$, $\Gamma=0.0035\,\omega_{\mathrm{TO}}\ \mathrm{cm^{-1}}$. The dashed curves correspond to a three-oscillator model, which accounts for a selective damping process involving the two-phonon band $TA(X)+LA(X)$ peaked at 357 cm⁻¹ [48]. The resolution (in $\boldsymbol{k}$-space) of our present apparatus

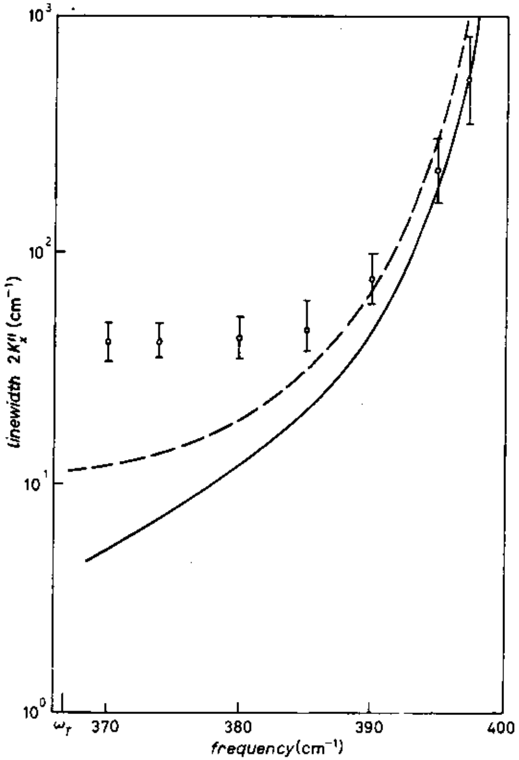

Fig. 10. – Frequency dependence of the $\boldsymbol{K}$-space line width $2K''(\omega)$.

is not yet large enough for us to deduce the true values of $K''(\omega)$ below $\omega=385\ \mathrm{cm^{-1}}$. This is mainly due to the sizable angular spread of the focused beams ω_1 and ω_2 (4 mrad). The same lack of accuracy in the same frequency region affects the measurement of the nonlinear optical susceptibility of the crystal $\chi^{(2)}(\omega)$. More accurate measurements of $\chi^{(2)}(\omega)$ in the reststrahl band and of $K''_x(\omega)$ with an apparatus having a 5 times larger resolution are presently in progress in our laboratory, for GaP an other semiconductors.

A technique similar to the one we have just described can be applied to the investigation of the exciton surface polaritons by the method of 4-wave mixing or by sum frequency generation (sect. **3**). Some numerical examples relative to the Z_3 exciton resonance in CuCl are given in [46].

Note added in proofs.

The nonlinear excitation of SP in the *C*-exciton reststrahl band in ZnO ($\hbar\omega_T = 3.421$ eV) has been recently achieved [49]. The field has been excited by second-harmonic generation and the (SP) UV radiation has been coupled out by the prism method (FTR).

REFERENCES

[1] N. Bloembergen: *Nonlinear Optics* (New York, N. Y., 1965). Throughout the present paper we shall make frequently use of some results reported in N. Bloembergen and P. S. Pershan: *Phys. Rev.*, **128**, 606 (1962).

[2] F. De Martini: *Phys. Lett.*, **30** A, 319, 547 (1969); *Phys. Rev. B*, **4**, 4556 (1971). The comment reported in ref. [43] of this paper is incorrect.

[3] Y. R. Shen: *Phys. Rev.*, **138**, A 1741 (1965).

[4] P. N. Butcher and T. P. McLean: *Proc. Phys. Soc.*, **81**, 219 (1963).

[5] C. H. Henry and C. G. B. Garrett: *Phys. Rev.*, **171**, 1058 (1968).

[6] R. Loudon: *Proc. Roy. Soc.*, A **275**, 218 (1963); *Rendiconti S.I.F.*, Course XLII, edited by R. Glauber (New York, N. Y., 1969).

[7] K. Huang: *Proc. Roy. Soc.*, A **208**, 352 (1951).

[8] C. Kittel: *Quantum Theory of Solids* (New York, N. Y., 1964), p. 42.

[9] W. L. Faust and C. H. Henry: *Phys. Rev. Lett.*, **17**, 1265 (1956); W. L. Faust, C. H. Henry and R. H. Eick: *Phys. Rev.*, **173**, 781 (1968).

[10] W. Heitler: *Quantum Theory of Radiation*. sect. **7** (Oxford, 1964).

[11] P. N. Butcher: *Nonlinear Optical Phenomena* (Columbus, O., 1965), p. 43.

[12] M. Abragam: *The Principles of Nuclear Magnetism* (Oxford, 1961).

[13] M. Goeppert-Mayer: *Ann. der Phys.*, **9**, 273 (1931).

[14] J. J. Hopfield, J. M. Worlock and K. Park: *Phys. Rev. Lett.*, **11**, 414 (1963).

[15] J. J. Hopfield: *Phys. Rev.*, **182**, 945 (1968).

[16] M. Born and E. Wolf: *Principles of Optics* (New York, N. Y., 1964), p. 14.

[17] J. A. Giordmaine: *Phys. Rev. Lett.*, **8**, 19 (1962).

[18] R. S. Knox: *Theory of Excitons* (New York, N. Y., 1963), p. 163.

[19] S. I. Pekar: *Žurn. Ėksp. Teor. Fiz.*, **33**, 1022 (1957); *Phys. Chem. Sol.*, **5**, 11 (1958).

[20] J. P. Coffinet and F. De Martini: *Phys. Rev. Lett.*, **22**, 60 (1969); *Phys. Rev. Lett.*, **22**, 752 (1969) (Erratum).

[21] E. Yablonovitch, C. Flytzanis and N. Bloembergen: *Phys. Rev. Lett.*, **29**, 864 (1972).

[22] J. J. Wynne: *Phys. Rev. Lett.*, **29**, 650 (1972).

[23] P. N. Butcher, R. Loudon and T. P. McLean: *Proc. Phys. Soc.*, **85**, 565 (1965).

[24] J. Ducuing: *Rendiconti S.I.F.*, Course XLII, edited by R. Glauber (New York,

[25] F. De Martini: *Nuovo Cimento*, **51** B, 16 (1967).

[26] F. De Martini: *Rendiconti S.I.F.*, Course LII, edited by E. Burstein (New York, N. Y., 1972).

[27] D. C. Hauseisen and H. Mahr: *Phys. Rev. Lett.*, **26**, 838 (1971).

[28] D. Frölich, B. Staginnus and E. Schönherr: *Phys. Rev. Lett.*, **19**, 1032 (1967).

[29] A. Bivas, C. Marange, J. B. Grun and C. Schwab: *Opt. Comm.*, **6**, 142 (1972).

[30] A. Gold: *Rendiconti S.I.F.*, Course XLII, edited by R. Glauber (New York, N.Y., 1969).

[31] S. D. Kramer, F. G. Parsons and N. Bloembergen: *Phys. Rev. B*, **9**, 1853 (1974); see also S. D. Kramer and N. Bloembergen: *Optical Properties of Highly Transparent Solids*, edited by S. S. Mitra and B. Bendow (New York, N.Y., 1975); S. Kramer: *Ph.D. Thesis* (Harvard University, 1976), unpublished; H. Lotem, R. Lynch, S. Kramer and N. Bloembergen: *Opt. Comm.* (1976), to be published.

[32] J. M. Aref'ev: *JETP Lett.*, **8**, 84 (1968); F. Zernicke and P. R. Berman: *Phys. Rev. Lett.*, **15**, 999 (1965); M. D. Martin and E. L. Thomas: *IEEE Journ. Quant. Elec.*, QE-**2**, 196 (1966); T. Yajima and K. Inoue: *IEEE Journ. Quant. Elec.*, QE-**5**, 140 (1969); D. W. Faries, K. A. Gehring, P. L. Richards and Y. R. Shen: *Phys. Rev.*, **180**, 363 (1969); F. Zernicke: *Phys. Rev. Lett.*, **22**, 931 (1969); S. Biraud and G. Chartier: *Phys. Lett.*, **30** A, 177 (1969).

[33] S. K. Kurtz and J. Giordmaine: *Phys. Rev. Lett.*, **22**, 192 (1969); J. M. Yarborough, S. S. Sussman, H. E. Puthoff, R. H. Pantell and C. Johnson: *Appl. Phys. Lett.*, **15**, 102 (1969).

[34] F. De Martini and J. Leroy: *Sol. State Comm.*, **9**, 1779 (1971).

[35] See work of V. Piesbergen: in *Semiconductors and Semimetals*, edited by Willardson and Beer, Vol. **2** (New York, N. Y., 1966).

[36] D. A. Kleinman and W. G. Spitzer: *Phys. Rev.*, **118**, 110 (1960).

[37] A. S. Barker: *Phys. Rev.*, **118**, 118 (1960).

[38] A. S. Barker: *Phys. Rev.*, **165**, 917 (1968).

[39] A. Sommerfeld: *Ann. der Phys.*, **28**, 665 (1909).

[40] U. Fano: *Journ. Opt. Soc. Amer.*, **31**, 213 (1941).

[41] E. Lifshitz and L. N. Rosenzweig: *Žurn. Ėksp. Teor. Fiz.*, **18**, 1012 (1948).

[42] *Proceedings of the Taormina Research Conference « Polaritons »*, edited by E. Burstein and F. De Martini (New York, N. Y., 1974).

[43] R. W. Gould and A. W. Trivelpiece: *Proc. Int. Electr. Eng. (London)*, B **105**, *Suppl.* **10**, 516 (1958).

[44] A. Otto: *Zeits. Phys.*, **216**, 398 (1968).

[45] N. Marschall and B. Fisher: *Phys. Rev. Lett.*, **28**, 811 (1972).

[46] F. De Martini and Y. R. Shen: *Phys. Rev. Lett.*, **36**, 216 (1976).

[47] F. De Martini, P. Mataloni, E. Palange and R. Y. Shen: to be published in *Phys. Rev. Lett.* and in *Proceedings of XIII International Conference on the Physics of Semiconductors* (Roma, 1976), to be published.

[48] A. S. Barker: *Phys. Rev.*, **165**, 917 (1968).

[49] M. Colocci, F. De Martini, S. Kohn and Y. R. Shen: to be published.